Article:
Lopez Garcia, M (2016) Stochastic Descriptors in an SIR Epidemic Model for Heterogeneous Individuals in Small Networks. Mathematical Biosciences, 271. pp. 42-61. ISSN 0025-5564

https://doi.org/10.1016/j.mbs.2015.10.010

Noname manuscript No.
(will be inserted by the editor)

Stochastic Descriptors in an SIR Epidemic Model for Heterogeneous Individuals in Small Networks

M. López-García

Received: date / Accepted: date

Abstract We continue here the work initiated in [13], and analyse an SIR epidemic model for the spread of an epidemic among the members of a small population of N individuals, defined in terms of a continuous-time Markov chain $\mathcal{X}$. We propose a structure by levels and sub-levels of the state space of the process $\mathcal{X}$, and present two different orders, Orders A and B, for states within each sub-level, which are related to a matrix and a scalar formalism, respectively, when developing our analysis. Stochastic descriptors regarding the length and size of an outbreak, the maximum number of individuals simultaneously infected during an outbreak, the fate of a particular individual within the population, and the number of secondary cases caused by a certain individual until he recovers, are deeply analysed. Our approach is illustrated by carrying out a set of numerical results regarding the spread of the nosocomial pathogen *Methicillin-resistant Staphylococcus Aureus* among the patients within an intensive care unit. In this application, our interest is in analysing the effectiveness of control strategies (the isolation of the patient initiating the outbreak and the proper room configuration of the intensive care unit) that intrinsically introduce heterogeneities among the members of the population.

Keywords Continuous-time Markov chain · Maximum number of infected individuals · Length and size of an outbreak · Individual fate · Nosocomial infections

Mathematics Subject Classification (2000) 92D30

M. López-García
Department of Applied Mathematics, School of Mathematics, University of Leeds, Leeds LS2 9JT, United Kingdom
E-mail: m.lopezgarcia@leeds.ac.uk

1 Introduction

The SIR (susceptible-infected-recovered) epidemic model is a well-known simple mathematical model, originally developed by Kermack and McKendrick [22] and widely analysed in the literature both from a deterministic [33] and a stochastic [2] perspective, which represents the spread of a disease throughout a population of individuals. These individuals can be, at any time instant, in three different states regarding the disease: susceptible (S), infected (I) or recovered (R). The process is then described, in the stochastic setting, as a continuous-time Markov chain (CTMC) $\{\mathbf{X}(t) = (I(t), R(t)) : \ t \geq 0\}$, where $I(t)$ and $R(t)$ amount to the total number of infected and recovered individuals, respectively, at time t. By considering a closed homogeneous population of N individuals, the total number of susceptible individuals at time t is given by $S(t) = N - I(t) - R(t)$, and the infinitesimal transition probabilities are described as

$$\mathbb{P}\left(\mathbf{X}(t+\Delta t) = (i', r') | \mathbf{X}(t) = (i, r)\right) = \begin{cases} \frac{\beta}{N} i(N-i-r)\Delta t + o(\Delta t), & \\ & \text{if } (i', r') = (i+1, r), \\ \gamma i \Delta t + o(\Delta t), & \\ & \text{if } (i', r') = (i-1, r+1), \\ 0, & \text{otherwise.} \end{cases}$$

This expression amounts to the consideration of a Poisson process with rate β for the infectious contacts made by a typical infected individual, and the assumption that any infected individual recovers after an exponentially distributed random time with mean $1/\gamma$, remaining then in state R indefinitely. During the last decades, different variants of this model have been considered addressing different applications in reality, for example: the $SIRS$ (susceptible-infected-recovered-susceptible) epidemic model considers that recovered individuals become susceptible again after an exponentially distributed time period, which may represent a temporary immunity that fades away; the consideration of latency periods where individuals are infected but not infectious yields the $SEIR$ (susceptible-exposed-infected-recovered) model; and SI_1I_2R-type models analyse epidemic processes where individuals can be in different infectious states, these states representing either two competing epidemics propagating within the same population [36] or different severity stages of the same infection [8]. We refer the reader to [10] for a detailed survey on stochastic epidemic models.

Increasingly research efforts within this topic are addressed to analyse how different external factors, such as vaccination strategies [12,19] or human behaviour [15] through information transmission [18,23], affect the propagation dynamics of the epidemic. On the other hand, different attempts have been also made to relax the homogeneous assumption for individuals within the population. Without any aim of an exhaustive enumeration, it is worth mentioning the work by Ball [6] where the author considers populations structured in households or groups of individuals, by Ball et al. [7] where there exist different types of individuals within the population, or cellular automata approaches

such as the work in [44], developed in order to deal with spatial, demographic or geographical patterns, as well as references therein. However, the consideration of a high degree of heterogeneity within the population has usually yielded the construction of appropriate networks or graphs in order to represent the contact structure of the individuals within the population when analysing the disease spread dynamics [30, Chapter 17]. In particular, the consideration of the stochastic SIR epidemic model within a graph where individuals are represented by nodes, and potential infectious contacts by edges theoretically yields a CTMC with 3^N states, which makes unfeasible any analytical or computational treatment [37] even for moderate values of N. Different approaches have been followed in the literature, and they take some advantage of the particular network structures arising in several applications in reality, such as scale-free networks [32] in problems related to social networks and the Internet, or small-world networks, introduced by Watts and Strogatz [43], which can be considered as a half-way point between lattices and random graphs. In general, analysing the dynamics of the spread of an epidemic within a network is a difficult problem from the analytical point of view, so that it is usual to follow Monte Carlo simulating approaches, or other approximating techniques such as the mean-field approximation [31,35], where individuals are classified and analysed in terms of their degree distribution, or the recently proposed N-intertwined approximation [42], originally developed for a SIS (susceptible-infected-susceptible) epidemic model and recently adapted for its SIR counterpart [46]; see [25] for a detailed comparison between these methods.

Our interest in this paper is in analysing the dynamics of the spread of the disease in a SIR epidemic model for an heterogeneous population, through the analysis of its corresponding exact 3^N-state CTMC. Moreover, we consider the case in which individuals can be infected due to external sources, which is an addition to the classic SIR setting. We provide here efficient procedures to analyse conveniently defined stochastic descriptors for the epidemic spread, being applicable in the relevant situation where N is small, which is the case in problems such as the epidemic spread throughout the members of a family [9, 17] or among the patients within an intensive care unit [4,11,14,28]. Although results developed in this paper are, theoretically, valid regardless the value of N, the computational nature of our procedures makes unfeasible their application once N exceeds small values (see Section 5 and Appendix C), and their interest beyond these values should be considered strictly mathematical. Thus, we alert the reader that our approach focuses on small populations or groups of individuals where the proper consideration of every heterogeneity within the population is more crucial than the introduction of additional individuals in the model which do not necessarily play a significant role. Moreover, while quantities exactly computed here may be efficiently approximated by means of stochastic simulations, our analysis contributes to shed some light on the space of states and the infinitesimal generator of networked Markovian epidemic processes, and on how these affect the study of different characteristics of interest from an analytical and computational perspective.

We point out here that the approach followed in this paper complements the work initiated in [13], where the application of a matrix formalism together with the usage of Laplace-Stieltjes transforms, probability generating functions, phase-type distributions [24, Chapter 2], level-dependent quasi-birth-and-death processes [24, Chapter 12] and auxiliary absorbing Markov chains are used when analysing a SIS epidemic model. Moreover, the particular application of this approach to the spread of the syndrome *Acute coryza* among the members of a family is studied in [13] by using empirical data of [9]. The matrix formalism followed in [13] is possible by means of considering a proper order of states within the space of states of the corresponding CTMC, which is similar to the order proposed in [39]. An alternative order when analysing the dynamics of the SIS epidemic model is the one considered in [42], which yields a particular fractal structure for the infinitesimal generator of the CTMC (see [42, Figures 2 and 3]), for which computational exploitation is an open question [42]. It is also worth mentioning the work in [35], where an exact expression for the infinitesimal generator is obtained for a general class of models representing spreading processes in multilayer complex networks.

In order to analyse the dynamics of the disease spread in the SIR epidemic model, we propose here both a scalar and a matrix formalism, implemented by means of two different orders for the state space of the CTMC under consideration. Under both formalisms, we define several stochastic descriptors when analysing the propagation dynamics during an outbreak. The interpretation of these descriptors, which are partially inspired in their applicability for the particular case of the spread of nosocomial infections within an intensive care unit, is illustrated here by carrying out a series of numerical results for analysing the spread of *Methicillin-resistant Staphylococcus Aureus* throughout the patients within an intensive care unit. Finally, we discuss about the convenience of using each formalism by taking into account not only their computational performance, but also their adaptability when variants of the SIR epidemic model are considered.

The paper is organised as follows. In Section 2, the Markovian process modeling the epidemic spread throughout the population is defined, and two different orders, termed Orders A and B, for states within the state space of this Markov chain are proposed. In Section 3, we define different stochastic descriptors of interest in our process for analysing the dynamics of the propagation of the infection within the population during an outbreak, and iterative schemes for computing related quantities are given in Appendix C. In Section 4, we illustrate our approach with an application to the spread of an epidemic among the patients within an intensive care unit, under the assumption that no discharge of patients occurs during the outbreak. Finally, some discussion is given in Section 5, where the impact of this assumption is also analysed. Standard notation used throughout the paper is presented in Appendix A, while an iterative procedure for computing the infinitesimal generator of the Markov chain under study is given in Appendix B.

2 Mathematical model

We consider throughout this paper a SIR epidemic model for the spread of an infection throughout the members of a small heterogeneous population of individuals. Let us consider a graph $\mathcal{G} = (\mathcal{N}, \mathcal{L})$ where $\mathcal{N} = \{1, \ldots, N\}$ is the set of vertices or nodes, representing $N > 0$ individuals within a population, and $\mathcal{L} \subseteq \mathcal{N} \times \mathcal{N}$ is the set of edges or links in the graph. In a general setting, we analyse the directed case, so that it is possible to have $(i, j) \in \mathcal{L}$ and $(j, i) \notin \mathcal{L}$. The link (i, j) represents some kind of interaction *from* individual i *towards* individual j, so that if individual i is infected at certain time instant, he can eventually infect j due to contact. Each edge (i, j) has a corresponding weight $\beta_{ij} \geq 0$ which represents the *amount of interaction* from i towards j, so that $\beta_{ij} = 0$ is equivalent to $(i, j) \notin \mathcal{L}$. These weights are stored in the *adjacency* matrix $\mathbf{B} = [\beta_{ij}]_{i,j \in \mathcal{N}}$, so that our assumption regarding a directed graph means here that $\mathbf{B}$ is not necessarily symmetric.

At time t, each individual (node) of the population can be in three possible states: susceptible (S), infected (I) or recovered (R). A susceptible node $i \in \mathcal{N}$ can eventually become infected due to:

1. An *external* source of infection (which amounts to, for example, individuals which have not been explicitly considered in the network). This occurs after an exponentially distributed random time with rate $\lambda_i \geq 0$.
2. An infectious contact with an infected individual within the network, $j \in \mathcal{N}$, which occurs after an exponentially distributed random time with rate $\beta_{ji} \geq 0$.

An infected node $i \in \mathcal{N}$ recovers after an exponentially distributed random time with rate $\gamma_i \geq 0$, acquiring immunity and remaining in this state indefinitely. Previous assumptions yield a CTMC $\mathcal{X} = \{\mathbf{X}(t) = (X_1(t), X_2(t), \ldots, X_N(t)) : t \geq 0\}$, where each random variable $X_i(t)$ represents the state of the individual i at time t, so that it can take values S, I or R. The space of states of $\mathcal{X}$ is then given by $\mathcal{S} = \{S, I, R\}^N$.

A detailed analysis of $\mathcal{X}$ requires to order states within $\mathcal{S}$. In this paper we propose two different orders for states within $\mathcal{S}$, Orders A and B, which permit the definition and subsequent analysis of stochastic descriptors of interest in Section 3, and the development of efficient matrix and scalar algorithms, respectively, for computing related quantities.

2.1 The state space: orders

For any state $\mathbf{x} \in \mathcal{S}$, we define sets of nodes $S(\mathbf{x}) = \{i \in \mathcal{N} : \mathbf{x}_i = S\}$, $I(\mathbf{x}) = \{i \in \mathcal{N} : \mathbf{x}_i = I\}$ and $R(\mathbf{x}) = \{i \in \mathcal{N} : \mathbf{x}_i = R\}$, and the states $S_j(\mathbf{x})$, $I_j(\mathbf{x})$ and $R_j(\mathbf{x})$ obtained from $\mathbf{x}$ by replacing $\mathbf{x}_j$ by S, I and R, respectively, for any $j \in \{1, \ldots, N\}$. Then, it is clear that $S_j(\mathbf{x}) = \mathbf{x}$ if and only if $j \in S(\mathbf{x})$, and similarly for $I_j(\mathbf{x})$ and $R_j(\mathbf{x})$. This notation permits to describe in a

precise and simple manner the non-null infinitesimal transition rates of $\mathcal{X}$ as

$$q_{\mathbf{x},\mathbf{y}} = \begin{cases} \lambda_j + \sum\limits_{i \in I(\mathbf{x})} \beta_{ij}, & \text{if } \mathbf{x}_j = S \text{ and } \mathbf{y} = I_j(\mathbf{x}), \\ \gamma_j, & \text{if } \mathbf{x}_j = I \text{ and } \mathbf{y} = R_j(\mathbf{x}), \\ 0, & \text{otherwise,} \end{cases} \tag{1}$$

for any node $i \in \{1, \ldots, N\}$. Eq. (1) follows from the fact that in the Markovian process $\mathcal{X}$, susceptible individuals are infected one at a time (which is related to $\mathbf{y} = I_j(\mathbf{x})$ in Eq. (1), representing the infection of individual j), and infected individuals are recovered one at a time (which is related to $\mathbf{y} = R_j(\mathbf{x})$ in Eq. (1), representing the recovery of individual j). For convenience, we from now on assume that every individual is able to recover from the disease, $\gamma_i > 0$ for all $i \in \{1, \ldots, N\}$. Since we are interested in the dynamics of the epidemic until no infected individual remains in the population (see Section 3), these are the cases in which our analysis is consistent; we refer the reader to Section 5 for some discussion regarding different situations.

In order to analyse $\mathcal{X}$, it is necessary to give some structure to $\mathcal{S}$. It has been recently shown the convenience of grouping states $\mathbf{x} \in \mathcal{S}$ in terms of the number of infected, susceptible or recovered individuals within $\mathbf{x}$ [13,39]. In particular, the labelling of states in [13], which focuses on the number of infected individuals for the SIS epidemic model, yields an elegant and efficient structure of the infinitesimal generator of $\mathcal{X}$ (see [13, Equation (2)] and [39, Section 2.1]). Thus, we suggest to structure the space of states as

$$\mathcal{S} = \bigcup_{r=0}^{N} L(r), \quad L(r) = \bigcup_{i=0}^{N-r} L(r;i), \tag{2}$$

where $L(r) = \{\mathbf{x} \in \mathcal{S} : \#R(\mathbf{x}) = r\}$, $L(r;i) = \{\mathbf{x} \in \mathcal{S} : \#R(\mathbf{x}) = r, \#I(\mathbf{x}) = i\}$, and where $\#A$ represents the cardinality of set A. Then,

$$J(r;i) = \#L(r;i) = \binom{N}{r|i}, \text{ and } J(r) = \#L(r) = \sum_{i=0}^{N-r} J(r;i) = \binom{N}{r},$$

for any $0 \leq r \leq N$, $0 \leq i \leq N - r$, where we make use of the notation

$$\binom{N}{r|i} = \binom{N}{r}\binom{N-r}{i} = \frac{N!}{r!i!(N-r-i)!}, \text{ and } \binom{N}{r} = \frac{N!}{r!(N-r)!}.$$

Since the space of states depends on the population size N, we propose for the rest of this section to use the notation $\mathcal{S}^{(N)}$, $L^{(N)}(r)$, $L^{(N)}(r;i)$, $J^{(N)}(r)$ and $J^{(N)}(r;i)$. The organisation by levels and sub-levels of $\mathcal{S}^{(N)}$ proposed in (2) and the infinitesimal transition rates given in (1) yield the infinitesimal generator $\mathbf{Q}(N)$ of $\mathcal{X}$. In particular, $\mathbf{Q}(N)$ depends on the particular population size N,

has dimensions $3^N \times 3^N$, and is given by

$$\begin{pmatrix} \mathbf{Q}_{0,0}(N) & \mathbf{Q}_{0,1}(N) & \mathbf{0}_{J^{(N)}(0)\times J^{(N)}(2)} & \cdots & \mathbf{0}_{J^{(N)}(0)\times J^{(N)}(N)} \\ \mathbf{0}_{J^{(N)}(1)\times J^{(N)}(0)} & \mathbf{Q}_{1,1}(N) & \mathbf{Q}_{1,2}(N) & \cdots & \mathbf{0}_{J^{(N)}(1)\times J^{(N)}(N)} \\ \mathbf{0}_{J^{(N)}(2)\times J^{(N)}(0)} & \mathbf{0}_{J^{(N)}(2)\times J^{(N)}(1)} & \mathbf{Q}_{2,2}(N) & \cdots & \mathbf{0}_{J^{(N)}(2)\times J^{(N)}(N)} \\ \vdots & \vdots & \vdots & \ddots & \vdots \\ \mathbf{0}_{J^{(N)}(N-1)\times J^{(N)}(0)} & \mathbf{0}_{J^{(N)}(N-1)\times J^{(N)}(1)} & \mathbf{0}_{J^{(N)}(N-1)\times J^{(N)}(2)} & \cdots & \mathbf{Q}_{N-1,N}(N) \\ \mathbf{0}_{J^{(N)}(N)\times J^{(N)}(0)} & \mathbf{0}_{J^{(N)}(N)\times J^{(N)}(1)} & \mathbf{0}_{J^{(N)}(N)\times J^{(N)}(2)} & \cdots & \mathbf{Q}_{N,N}(N) \end{pmatrix}. \tag{3}$$

We point out here that $L^{(N)}(N) = \{(R, \ldots, R)\}$ so that $\mathbf{Q}_{N,N}(N) = 0$ and $J^{(N)}(N) = 1$. The bidiagonal-by-blocks structure of $\mathbf{Q}(N)$ becomes clear by noting that, from a state $\mathbf{x} \in L^{(N)}(r) \subset \mathcal{S}^{(N)}$, the possible transitions are towards either states in $L^{(N)}(r)$ (if an infection occurs) or states in $L^{(N)}(r+1)$ (if a recovery occurs). Then, each block $\mathbf{Q}_{r,r'}(N)$ for $r' \in \{r, r+1\}$ contains, in an ordered manner, the infinitesimal transition rates for transitions from states in $L^{(N)}(r)$ to states in $L^{(N)}(r')$. Moreover, from a state $\mathbf{x} \in L^{(N)}(r;i) \subset L^{(N)}(r)$, possible transitions are towards states in $L^{(N)}(r;i+1)$ or in $L^{(N)}(r+1;i-1)$, so that sub-blocks $\mathbf{Q}_{r,r}(N)$ and $\mathbf{Q}_{r,r+1}(N)$ are given by

$$\mathbf{Q}_{r,r}(N) = \begin{pmatrix} \mathbf{Q}_{r,r}^{0,0}(N) & \mathbf{Q}_{r,r}^{0,1}(N) & \mathbf{0} & \cdots & \mathbf{0} \\ \mathbf{0} & \mathbf{Q}_{r,r}^{1,1}(N) & \mathbf{Q}_{r,r}^{1,2}(N) & \cdots & \mathbf{0} \\ \mathbf{0} & \mathbf{0} & \mathbf{Q}_{r,r}^{2,2}(N) & \cdots & \mathbf{0} \\ \vdots & \vdots & \vdots & \ddots & \vdots \\ \mathbf{0} & \mathbf{0} & \mathbf{0} & \cdots & \mathbf{Q}_{r,r}^{N-r-1,N-r}(N) \\ \mathbf{0} & \mathbf{0} & \mathbf{0} & \cdots & \mathbf{Q}_{r,r}^{N-r,N-r}(N) \end{pmatrix}, \ 0 \le r \le N,$$

$$\mathbf{Q}_{r,r+1}(N) = \begin{pmatrix} \mathbf{0} & \mathbf{0} & \cdots & \mathbf{0} \\ \mathbf{Q}_{r,r+1}^{1,0}(N) & \mathbf{0} & \cdots & \mathbf{0} \\ \mathbf{0} & \mathbf{Q}_{r,r+1}^{2,1}(N) & \cdots & \mathbf{0} \\ \vdots & \vdots & \ddots & \vdots \\ \mathbf{0} & \mathbf{0} & \cdots & \mathbf{0} \\ \mathbf{0} & \mathbf{0} & \cdots & \mathbf{Q}_{r,r+1}^{N-r,N-r-1}(N) \end{pmatrix}, \quad 0 \le r \le N-1,$$

where dimensions of null sub-blocks $\mathbf{0}$ are omitted. Each sub-block $\mathbf{Q}_{r,r'}^{i,i'}(N)$ contains, in an ordered manner, the infinitesimal transition rates for transitions from states in $L^{(N)}(r;i)$ to states in $L^{(N)}(r';i')$, for $(r',i') \in \{(r,i),(r,i+1),(r+1,i-1)\}$.

Once the general structure of $\mathbf{Q}(N)$ is in hand, obtaining explicit expressions for sub-blocks $\mathbf{Q}_{r,r'}^{i,i'}(N)$ requires to define a particular order for the states inside each sub-level $L^{(N)}(r;i)$, for $0 \le r \le N$, $0 \le i \le N-r$. Regardless of the order considered, sub-blocks $\mathbf{Q}_{r,r}^{i,i}(N)$ are diagonal matrices with elements $-q_{\mathbf{x}} = q_{\mathbf{x},\mathbf{x}} = -(\sum_{j\in S(\mathbf{x})}(\lambda_j + \sum_{i\in I(\mathbf{x})}\beta_{ij}) + \sum_{i\in I(\mathbf{x})}\gamma_i)$ within the diagonal, so that $\mathbf{Q}(N)$ is conservative.

In Subsection 2.1.1 we propose the reverse lexicographic order (Order A) for states inside each sub-level $L^{(N)}(r;i)$. This order, inspired in the order

proposed in [13] for the SIS epidemic model, permits an elegant iterative construction of the infinitesimal generator $\mathbf{Q}(N)$. By giving a pivotal role to the last individual N, this order has the advantage of allowing us the construction of efficient matrix iterative procedures when studying stochastic descriptors defined in Section 3. Moreover, the matrix approach implemented in Section 3 and Appendix C by means of Order A, allows one to adapt arguments presented in this paper to different epidemic models (e.g., the SIS epidemic model [13], or an especial version of the SIRS epidemic model in our discussion in Section 5).

On the other hand, in order to work with a scalar formalism when analysing stochastic descriptors in Section 3, one may need to be able to localise each state $\mathbf{x}$ within its sub-level $L^{(N)}(r;i)$. Although this might be possible to be done by using Order A, we propose here to follow, to this end, the more *natural* lexicographic order (Order B) for states within each sub-level, so that Eq. (4) is obtained in Subsection 2.1.2. See Section 5 and Appendix C for some discussion about the convenience of following each approach.

2.1.1 Reverse lexicographic order: Order A

In this subsection, Order A gives a crucial role to the last individual (the Nth node) in the population. In particular, Order A consists of ordering states $\mathbf{x} \in L^{(N)}(r;i)$, for $0 \leq r \leq N$ and $0 \leq i \leq N-r$, following steps (i)-(iv):

(i) To translate states of $\mathcal{S}^{(N)} = \{S, I, R\}^N$ into states of $\{0, 1, 2\}^N$ with $S \equiv 0$, $I \equiv 1$ and $R \equiv 2$.
(ii) To order states within $L^{(N)}(r;i)$ in a lexicographical manner.
(iii) To turn over states $(x_1, \ldots, x_N) \in L^{(N)}(r;i) \to (x_N, \ldots, x_1) \in L^{(N)}(r;i)$.
(iv) To translate again states of $\{0, 1, 2\}^N$ into states of $\mathcal{S}^{(N)} = \{S, I, R\}^N$.

For example, order of states inside level $L^{(4)}(2;1)$ is given in Figure 1. Order A defined by steps (i)-(iv) for states within each sub-level $L^{(N)}(r;i)$ yields an iterative construction of $\mathbf{Q}(N)$. This procedure (Appendix B) starts with the trivial matrix $\mathbf{Q}(1)$ and computes $\mathbf{Q}(M)$ from $\mathbf{Q}(M-1)$ until reaching the desired value $M = N$. This iterative scheme can be constructed thanks of Order A properly reflecting the relationship between levels $L^{(N)}(r)$ and sub-levels $L^{(N)}(r;i)$ and levels $L^{(N-1)}(r')$ and sub-levels $L^{(N-1)}(r';i')$.

2.1.2 Lexicographic order: Order B

In Order B, we order states in $L^{(N)}(r;i)$ lexicographically, with the identification $S \equiv 0$, $I \equiv 1$ and $R \equiv 2$. That is, sub-level $L^{(N)}(r;i)$ is ordered

Unordered States		*Ordered States*
(R,R,I,S)		(R,R,I,S)
(R,R,S,I)		(R,I,R,S)
(R,I,R,S)		(I,R,R,S)
(R,S,R,I)		(R,R,S,I)
(R,I,S,R)	(i)	(R,S,R,I)
(R,S,I,R)	$\Rightarrow$	(S,R,R,I)
(I,R,R,S)		(R,I,S,R)
(S,R,R,I)		(I,R,S,R)
(I,R,S,R)		(R,S,I,R)
(S,R,I,R)		(S,R,I,R)
(I,S,R,R)		(I,S,R,R)
(S,I,R,R)		(S,I,R,R)

$(2,2,1,0)$	$(0,1,2,2)$	$(2,2,1,0)$
$(2,2,0,1)$	$(0,2,1,2)$	$(2,1,2,0)$
$(2,1,2,0)$	$(0,2,2,1)$	$(1,2,2,0)$
$(2,0,2,1)$	$(1,0,2,2)$	$(2,2,0,1)$
$(2,1,0,2)$	$(1,2,0,2)$	$(2,0,2,1)$
$(2,0,1,2)$	$(1,2,2,0)$	$(0,2,2,1)$
$(1,2,2,0)$	$(2,0,1,2)$	$(2,1,0,2)$
$(0,2,2,1)$	$(2,0,2,1)$	$(1,2,0,2)$
$(1,2,0,2)$	$(2,1,0,2)$	$(2,0,1,2)$
$(0,2,1,2)$	$(2,1,2,0)$	$(0,2,1,2)$
$(1,0,2,2)$	$(2,2,0,1)$	$(1,0,2,2)$
$(0,1,2,2)$	$(2,2,1,0)$	$(0,1,2,2)$

(ii) $\Rightarrow$ (iii) $\Rightarrow$ (iv) $\Rightarrow$

Fig. 1 Order of states within sub-level $L^{(4)}(2;1)$

as

Position	*State* $\mathbf{x}$											
in $L^{(N)}(r;i)$	x_1	$\ldots$	x_{N-r-i}	$x_{N-r-i+1}$	$\cdots$	x_{N-r-1}	x_{N-r}	x_{N-r+1}	x_{N-r+2}	$\cdots$	x_{N-1}	x_N
0	0	$\ldots$	0	1	$\ldots$	1	1	2	2	$\ldots$	2	2
1	0	$\ldots$	0	1	$\ldots$	1	2	1	2	$\ldots$	2	2
2	0	$\ldots$	0	1	$\ldots$	1	2	2	1	$\ldots$	2	2
$\vdots$	$\vdots$	$\vdots$	$\vdots$	$\vdots$	$\vdots$	$\vdots$	$\vdots$	$\vdots$	$\vdots$	$\vdots$	$\vdots$	$\vdots$
r	0	$\ldots$	0	1	$\ldots$	1	2	2	2	$\ldots$	2	1
$r+1$	0	$\ldots$	0	1	$\ldots$	2	1	1	2	$\ldots$	2	2
$r+2$	0	$\ldots$	0	1	$\ldots$	2	1	2	1	$\ldots$	2	2
$\vdots$	$\vdots$	$\vdots$	$\vdots$	$\vdots$	$\vdots$	$\vdots$	$\vdots$	$\vdots$	$\vdots$	$\vdots$	$\vdots$	$\vdots$

The localisation of a particular state $\mathbf{x}$ inside $L^{(N)}(r;i)$ is possible when following Order B. In particular, for any state $\mathbf{x} \in L^{(N)}(r;i)$ we may define $Pos_r^i(\mathbf{x})$ as its position within $L^{(N)}(r;i)$. Then, since sub-level $L^{(N)}(r;i)$ consists of $J^{(N)}(r;i) = \binom{N}{r|i}$ states lexicographically ordered, state $(0,\ldots,0,1,\ldots,1,2,\ldots,2)$ is in position 0 within $L^{(N)}(r;i)$ while state $(2,\ldots,2,1,\ldots,1,0,\ldots,0)$ is in position $J^{(N)}(r;i)-1$. For obtaining $Pos_r^i(\mathbf{x})$ for any state $\mathbf{x} \in L^{(N)}(r;i)$, we note that this state can be reexpressed as a two-arrays set containing the positions of digits 1 and 2 as

$$\mathbf{x} \equiv \{(a_1,\ldots,a_i),(b_1,\ldots,b_r)\}.$$

That is, values in $(a_1,\ldots,a_i)$ represent those individuals who are infected according to state $\mathbf{x}$, while values in $(b_1,\ldots,b_r)$ represent those individuals who are recovered according to state $\mathbf{x}$. Arrays $(a_1,\ldots,a_i)$ and $(b_1,\ldots,b_r)$ are always considered ordered, and states with no infected individuals or no recovered individuals are represented by $\{(),(b_1,\ldots,b_r)\}$ and $\{(a_1,\ldots,a_i),()\}$, respectively. Then, given a sub-level $L^{(N)}(r;i)$, state $\{(N-r-i+1,N-r-i+2,\ldots,N-r),(N-r+1,\ldots,N)\}$ is in position 0, while state $\{(r+1,\ldots,r+i),(1,\ldots,r)\}$ is in the last position $J^{(N)}(r;i)-1$. Given an arbitrary state $\mathbf{x} = \{(a_1,\ldots,a_i),(b_1,\ldots,b_r)\} \in L^{(N)}(r;i)$, we define its associated list of

indices $(j_1,\ldots,j_r)$ such that $a_{j_k-1} < b_k < a_{j_k}$, $j_k \in \{1,\ldots,i+1\}$ for all $k \in \{1,\ldots,r\}$ (with special cases $j_k = 1$ if $b_k < a_1$ and $j_k = i+1$ if $b_k > a_i$). Then, the position $Pos_r^i(\mathbf{x})$ of $\mathbf{x}$ within $L^{(N)}(r;i)$ is given by

$$Pos_r^i(\mathbf{x}) = \sum_{k=0}^{r}\left(\sum_{l=j_k}^{j_{k+1}-1}\binom{N-a_l}{r-k|i-l+1}\right) + \sum_{k=1}^{r}\left(\binom{N-b_k}{r-k+1|i-(j_k-1)} + \binom{N-b_k}{r-k+1|i-j_k}\right), \tag{4}$$

where empty summations $\sum_a^b$ with $a > b$ and binomial coefficients $\binom{a}{b|c}$ with $b + c > a$ are considered null, and where $j_0 = 1$ and $j_{r+1} = i+1$ are implicitly defined for convenience. The proof of Eq. (4), which is omitted here, is based in combinatorial arguments for computing the number of states $\mathbf{y} = \{(\tilde{a}_1,\ldots,\tilde{a}_i),(\tilde{b}_1,\ldots,\tilde{b}_r)\}$ preceding $\mathbf{x}$ within $L^{(N)}(r;i)$.

For example, state $\mathbf{x} = (0,1,1,2,0,1,1,2,2,1) \in L^{(10)}(3;5)$ can be reexpressed as $\mathbf{x} = \{(2,3,6,7,10),(4,8,9)\}$, with associated list of indices $(j_1,j_2,j_3) = (3,5,5)$ since $a_2 < b_1 < a_3$, $a_4 < b_2 < a_5$ and $a_4 < b_3 < a_5$. Then, $L^{(10)}(3;5)$ contains $J^{(10)}(3;5) = 2520$ states, state $(0,0,1,1,1,1,1,2,2,2)$ is in position 0 in $L^{(10)}(3;5)$ and state $(2,2,2,1,1,1,1,1,0,0)$ is in position $J^{(10)}(3;5)-1 = 2519$. Finally, following the Order B, state $\mathbf{x} = (0,1,1,2,0,1,1,2,2,1)$ is in position $Pos_r^i(\mathbf{x}) = 173$ within $L^{(10)}(3;5)$ computed from Eq. (4).

3 Stochastic descriptors

In this section, we focus on four particular stochastic descriptors that provide information about the propagation dynamics of the epidemic throughout the network, and they are related to an outbreak. An outbreak of the epidemic is defined as the time interval since a particular individual is infected (and then, propagation of the disease begins from a state $\mathbf{x} \in L^{(N)}(0;1)$) until no infected individuals remain in the population (arrival to a state $\mathbf{y} \in L^{(N)}(r;0)$ for some $r \in \{1,\ldots,N\}$). For a particular outbreak starting in $\mathbf{x} \in L^{(N)}(0;1)$, we define the following descriptors:

- Population descriptors:
  1. *Length and size of the outbreak*: if every individual is infected during the outbreak, the state at the end of the outbreak is trivially $(R,\ldots,R)$. If only a sub-set of individuals is infected during the outbreak, then the state at the end of the outbreak is $\mathbf{y} \in L^{(N)}(r;0)$ for some value $1 \leq r \leq N-1$. Our interest is in the total duration of the outbreak and the number of recovered individuals when it ends.
  2. *Maximum number of individuals simultaneously infected during the outbreak*: this descriptor permits to measure the amount of resources needed when dealing with the epidemic.
- Individual descriptors:

3. *Probability of a particular node suffering the disease during the outbreak, type of infection suffered and time until this occurs*: these descriptors permit to analyse individual fate (whether a particular individual is infected or not during the outbreak, as well as whether this infection is directly caused by an external source or by a contact within the network). They allow us to understand the susceptibility of each individual within the network to the network itself and to external sources of infection, so that quantitatively-based decisions could be made under individual basis regarding vaccination and/or isolation strategies.
4. *Exact reproduction number of each node*: this measures the number of secondary infections caused by a particular individual until he recovers [3,34]. This descriptor provides information on the infectiousness of each particular individual within the population.

We point out here that an outbreak finishes when $\mathcal{X}$ arrives to a state $\mathbf{y} \in L^{(N)}(r;0)$ for some $r \in \{1,\dots,N\}$, which may or may not be an absorbing state in $\mathcal{X}$ (depending on the particular values of parameters β_{ij}, λ_i and γ_i). Descriptors 1-4 may be analysed in an alternative manner if they were defined for the total time period until the process reaches any absorbing state $\mathbf{y} \in L^{(N)}(r;0)$ for some $r \in \{1,\dots,N\}$. In this situation, arguments in Section 3 may be adapted, which is out of the scope of this paper.

3.1 Length and final size of an outbreak

Since the population size N is fixed, the superscript N is removed from notation from now on. We are interested in the dynamics of the process until no infected individuals remain in the population, hence the state space is split in

$$\mathcal{S} = \mathcal{C} \cup \mathcal{C}_0,$$

where $\mathcal{C} = \{\mathbf{x} \in \mathcal{S} : \ \#I(\mathbf{x}) \geq 1\} = \cup_{r=0}^{N} \cup_{i=1}^{N-r} L(r;i)$ and $\mathcal{C}_0 = \{\mathbf{x} \in \mathcal{S} : \#I(\mathbf{x}) = 0\} = \cup_{r=0}^{N} L(r;0)$. We define the random variable

$$T_{\mathbf{x}} = \textit{“Time until the process reaches, for the first time, the subset } \mathcal{C}_0\textit{, given that the current state of } \mathcal{X} \textit{ is } \mathbf{x} \in \mathcal{C}\textit{”},$$

which amounts to the length of the outbreak when $\mathbf{x}$ is the current state. The size of the outbreak can be analysed in terms of the random variable

$$R_{\mathbf{x}} = \textit{“Number of recovered individuals at the end of the outbreak, given that the current state of } \mathcal{X} \textit{ is } \mathbf{x} \in \mathcal{C}\textit{”},$$

taking values among $\{\#I(\mathbf{x}) + \#R(\mathbf{x}), \dots, N\}$.

In order to study these random variables, we analyse the auxiliary process $\tilde{\mathcal{X}}$ defined over $\tilde{\mathcal{S}} = \mathcal{C} \cup \{1\} \cup \{2\} \cup \cdots \cup \{N\}$, where states $\bar{R} \in \{1,\dots,N\}$ are absorbing macro-states in the CTMC $\tilde{\mathcal{X}}$, and they are constructed from $\mathcal{S}$ by lumping all the states within $L(1;0)$, $L(2;0)$, $\dots$, and $L(N;0)$, respectively.

That is, the absorption of the process $\tilde{\mathcal{X}}$ into a macro-state $\bar{R} \in \{1, \ldots, N\}$ represents the finalisation of the outbreak in the original process, with $\bar{R}$ final recovered individuals. Transitions between states in $\mathcal{C}$ for the process $\tilde{\mathcal{X}}$ are maintained from those ones in $\mathcal{X}$. Transitions from states in $\mathcal{C}$ towards states in $L(r;0) \subset \mathcal{C}_0$ in the original process are translated into transitions from states in $\mathcal{C}$ towards the macro-state $\bar{R} = r$ for process $\tilde{\mathcal{X}}$.

From the previous construction we note that the time $T_{\mathbf{x}}$ until the end of the outbreak in the original process, given an initial state $\mathbf{x} \in \mathcal{C}$, corresponds to the time until absorption in $\{1\} \cup \cdots \cup \{N\}$ in the auxiliary process. This absorption time is well-known to follow a continuous phase-type (PH_c) distribution; see e.g. [24, Chapter 2]. Then, its probability density function can be obtained in terms of the matrix exponential of a particular sub-matrix of the infinitesimal generator of $\tilde{\mathcal{X}}$ that, at the same time, can be obtained from the infinitesimal generator of $\mathcal{X}$ iteratively computed in Appendix B. However, the computation of a matrix exponential is not possible in general in an exact way, and its numerical approximation is computationally expensive [29]. Thus, we propose here to analyse the Laplace-Stieltjes transforms of $T_{\mathbf{x}}$ by making use of the particular structure by levels and sub-levels of $\mathcal{C}$, permitting to study in a joint manner the random variables of interest $T_{\mathbf{x}}$ and $R_{\mathbf{x}}$.

We note that, for any $\bar{R} \in \{1, \ldots, N\}$, the absorption probability $\mathbb{P}(R_{\mathbf{x}} = \bar{R})$ equals the probability $\mathbb{P}(T_{\mathbf{x}}(\bar{R}) < \infty)$ where $T_{\mathbf{x}}(\bar{R})$ is defined as

$$T_{\mathbf{x}}(\bar{R}) = \text{“}\textit{Time until absorption of process } \tilde{\mathcal{X}} \textit{ into the macro-state } \bar{R}\textit{, given that the current state of } \tilde{\mathcal{X}} \textit{ is } \mathbf{x} \in \mathcal{C}\text{”}.$$

Since absorption of $\tilde{\mathcal{X}}$ may occur into any of the absorbing states $\bar{R} \in \{1, \ldots, N\}$, the random variable $T_{\mathbf{x}}(\bar{R})$ is infinite with positive probability, and $T_{\mathbf{x}}(\bar{R}) < \infty$ is equivalent to the absorption exactly occurring into $\bar{R}$. Thus, we consider the Laplace-Stieltjes transforms

$$\phi_{\mathbf{x}}(\bar{R}; z) = E\left[e^{-zT_{\mathbf{x}}(\bar{R})} 1_{\{T_{\mathbf{x}}(\bar{R}) < \infty\}}\right], \quad \Re(z) \geq 0,$$

for any $\mathbf{x} \in \mathcal{C}$, $\bar{R} \in \{1, \ldots, N\}$, where $1_{\{T_{\mathbf{x}}(\bar{R}) < \infty\}}$ is a random variable taking the value 1 if $T_{\mathbf{x}}(\bar{R}) < \infty$ and 0 otherwise, so that the previous Laplace-Stieltjes transforms are restricted to the sample paths verifying $T_{\mathbf{x}}(\bar{R}) < \infty$. The moments of $T_{\mathbf{x}}(\bar{R})$, $m_{\mathbf{x}}^{(l)}(\bar{R}) = E[(T_{\mathbf{x}}(\bar{R}))^l 1_{\{T_{\mathbf{x}}(\bar{R}) < \infty\}}]$, are obtained as

$$m_{\mathbf{x}}^{(l)}(\bar{R}) = \frac{d^l}{dz^l} \phi_{\mathbf{x}}(\bar{R}; z)\bigg|_{z=0}, \quad l \geq 1, \quad \mathbf{x} \in \mathcal{C}.$$

The random variables $T_{\mathbf{x}}$ and $R_{\mathbf{x}}$, can be then analysed in terms of

$$\begin{aligned}
\mathbb{P}(R_{\mathbf{x}} = \bar{R}) = \mathbb{P}(T_{\mathbf{x}}(\bar{R}) < \infty) &= \phi_{\mathbf{x}}(\bar{R}; 0), \quad \mathbf{x} \in \mathcal{C}, \quad \bar{R} \in \{1, \ldots, N\}, \\
\phi_{\mathbf{x}}(z) = E\left[e^{-zT_{\mathbf{x}}}\right] &= \sum_{\bar{R}=1}^{N} \phi_{\mathbf{x}}(\bar{R}; z), \quad \Re(z) \geq 0, \quad \mathbf{x} \in \mathcal{C}, \qquad (5) \\
m_{\mathbf{x}}^{(l)} = E\left[(T_{\mathbf{x}})^l\right] &= \sum_{\bar{R}=1}^{N} m_{\mathbf{x}}^{(l)}(\bar{R}), \quad l \geq 1,
\end{aligned}$$

and the computation of the probability density function of $T_{\mathbf{x}}$ could be obtained by numerical inversion of the transform $\phi_{\mathbf{x}}(z)$; see e.g. [1]. We point out that this is well-known to be computationally expensive as well, since it is comparable to the computation of the matrix exponential of a sub-matrix of the infinitesimal generator, which on the other hand could be achieved by efficient methods [21,38]. We pursue here to compute the different moments $m_{\mathbf{x}}^{(l)}(\bar{R})$ and probabilities $\mathbb{P}(R_{\mathbf{x}} = \bar{R})$, by analysing first the transforms $\phi_{\mathbf{x}}(\bar{R}; z)$, and refer the reader to [24, Section 2.8] and references therein for a discussion on the different methods for computing the probability density function of a phase-type distribution, where the *uniformization* method is presented as a particularly suitable solution.

The computation of restricted transforms $\phi_{\mathbf{x}}(\bar{R}; z)$, for a fixed value $\bar{R} \in \{1, \ldots, N\}$, can be accomplished by following the first-step argument

$$\phi_{\mathbf{x}}(\bar{R}; z) = \sum_{j \in S(\mathbf{x})} \frac{\lambda_j + \sum\limits_{k \in I(\mathbf{x})} \beta_{kj}}{z + q_{\mathbf{x}}} \phi_{I_j(\mathbf{x})}(\bar{R}; z) + \sum_{k \in I(\mathbf{x})} \frac{\gamma_k}{z + q_{\mathbf{x}}} \phi_{R_k(\mathbf{x})}(\bar{R}; z), \tag{6}$$

for any $\mathbf{x} \in \mathcal{C}$, where $R_k(\mathbf{x}) \equiv \bar{R}'$ if $\mathbf{x} \in L(\bar{R}' - 1; 1)$ and $\mathbf{x}_k = 1$, for any $\bar{R}' \in \{1, \ldots, N\}$. Eq. (6), for a given fixed value $\bar{R} \in \{1, \ldots, N\}$, yields a finite system of equations that relates the restricted transforms $\phi_{\mathbf{x}}(\bar{R}; z)$ for states in $\mathcal{C}$, with the boundary conditions $\phi_{\bar{R}'}(\bar{R}; z) = 0$ for $\bar{R}' \neq \bar{R}$ with $\bar{R}' \in \{1, \ldots, N\}$, $\phi_{\bar{R}}(\bar{R}; z) = 1$, and $\phi_{\mathbf{x}}(\bar{R}; z) = 0$, for any $\mathbf{x} \in \mathcal{C}$ with $\#I(\mathbf{x}) + \#R(\mathbf{x}) > \bar{R}$. This system of equations can be written in matrix form as

$$\mathbf{g}(\bar{R}; z) = \mathbf{A}(\bar{R}; z)\mathbf{g}(\bar{R}; z) + \mathbf{a}(\bar{R}; z), \tag{7}$$

where restricted transforms are stored in the column vector $\mathbf{g}(\bar{R}; z)$, which is structured as

$$\mathbf{g}(\bar{R}; z) = \begin{pmatrix} \mathbf{g}_0(\bar{R}; z) \\ \mathbf{g}_1(\bar{R}; z) \\ \vdots \\ \mathbf{g}_{\bar{R}-1}(\bar{R}; z) \end{pmatrix}, \ \mathbf{g}_r(\bar{R}; z) = \begin{pmatrix} \mathbf{g}_r^1(\bar{R}; z) \\ \mathbf{g}_r^2(\bar{R}; z) \\ \vdots \\ \mathbf{g}_r^{\bar{R}-r}(\bar{R}; z) \end{pmatrix}, \ 0 \leq r \leq \bar{R} - 1. \tag{8}$$

Matrix $\mathbf{A}(\bar{R}; z)$ has the same bidiagonal-by-blocks structure than $\mathbf{Q}(N)$ in (3), where quantities $J^{(N)}(r)$ are replaced by $\bar{J}(r) = \#\bar{L}(r) = \#\{\mathbf{x} \in \mathcal{C} : \#I(\mathbf{x}) + \#R(\mathbf{x}) \leq \bar{R}\} = \sum_{i=1}^{\bar{R}-r} \binom{N}{r|i}$, and sub-matrices $\mathbf{Q}_{r,r'}(N)$ are replaced by sub-matrices

$$\mathbf{A}_{r,r}(\bar{R}; z) = \begin{pmatrix} \mathbf{0} & \mathbf{A}_{r,r}^{1,2}(z) & \mathbf{0} & \ldots & \mathbf{0} & \mathbf{0} \\ \mathbf{0} & \mathbf{0} & \mathbf{A}_{r,r}^{2,3}(z) & \ldots & \mathbf{0} & \mathbf{0} \\ \mathbf{0} & \mathbf{0} & \mathbf{0} & \ldots & \mathbf{0} & \mathbf{0} \\ \vdots & \vdots & \vdots & \ddots & \vdots & \vdots \\ \mathbf{0} & \mathbf{0} & \mathbf{0} & \ldots & \mathbf{0} & \mathbf{A}_{r,r}^{\bar{R}-r-1,\bar{R}-r}(z) \\ \mathbf{0} & \mathbf{0} & \mathbf{0} & \ldots & \mathbf{0} & \mathbf{0} \end{pmatrix}, \quad 0 \leq r \leq \bar{R} - 1,$$

$$\mathbf{A}_{r,r+1}(\bar{R};z)=\begin{pmatrix}\mathbf{0} & \mathbf{0} & \dots & \mathbf{0} & \mathbf{0}\\ \mathbf{A}_{r,r+1}^{2,1}(z) & \mathbf{0} & \dots & \mathbf{0} & \mathbf{0}\\ \mathbf{0} & \mathbf{A}_{r,r+1}^{3,2}(z) & \dots & \mathbf{0} & \mathbf{0}\\ \vdots & \vdots & \ddots & \vdots & \vdots\\ \mathbf{0} & \mathbf{0} & \dots & \mathbf{A}_{r,r+1}^{\bar{R}-r-1,\bar{R}-r-2}(z) & \mathbf{0}\\ \mathbf{0} & \mathbf{0} & \dots & \mathbf{0} & \mathbf{A}_{r,r+1}^{\bar{R}-r,\bar{R}-r-1}(z)\end{pmatrix},$$

for $0\leq r\leq \bar{R}-2$. Sub-matrices $\mathbf{A}_{r,r'}^{i,i'}(z)$ are obtained by dividing each $\mathbf{x}$th row of sub-matrices $\mathbf{Q}_{r,r'}^{i,i'}(N)$ of the infinitesimal generator by $z+q_{\mathbf{x}}$. Finally, $\mathbf{a}(\bar{R};z)=\left(\mathbf{0}^T,\dots,\mathbf{0}^T,(\mathbf{A}_{\bar{R}-1,\bar{R}}^{1,0}(z)\mathbf{e}_{J(\bar{R};0)})^T\right)^T$.

The particular structure of $\mathbf{A}(\bar{R};z)$ can be used for solving (7) by backward substitution, so that Algorithm 1M (Part 1) is obtained and described in Appendix C. Since $\mathbb{P}(R_{\mathbf{x}}=\bar{R})=\phi_{\mathbf{x}}(\bar{R};0)$ from (5), the probability mass function of $R_{\mathbf{x}}$ is stored in the $\mathbf{x}$th row of vector $\mathbf{g}_r^i(\bar{R};z)$, where $\mathbf{x}\in L(r;i)$ and we vary $\bar{R}\in\{1,\dots,N\}$. In particular, transforms corresponding to initial states representing the beginning of an outbreak are stored within $\mathbf{g}_0^1(\bar{R};z)$.

Every lth order restricted moment of $T_{\mathbf{x}}(\bar{R})$ can be obtained by successive differentiation of Eq. (6). In particular, this yields

$$m_{\mathbf{x}}^{(l)}(\bar{R})=\sum_{j\in S(\mathbf{x})}\frac{\lambda_j+\sum\limits_{k\in I(\mathbf{x})}\beta_{kj}}{q_{\mathbf{x}}}m_{I_j(\mathbf{x})}^{(l)}(\bar{R})+\sum_{k\in I(\mathbf{x})}\frac{\gamma_k}{q_{\mathbf{x}}}m_{R_k(\mathbf{x})}^{(l)}(\bar{R})+\frac{l}{q_{\mathbf{x}}}m_{\mathbf{x}}^{(l-1)}(\bar{R}),\quad l\geq 1, \tag{9}$$

with $m_{\mathbf{x}}^{(0)}(\bar{R})=\phi_{\mathbf{x}}(\bar{R};0)$. These moments can be stored in $\mathbf{m}^{(l)}(\bar{R})=(\mathbf{m}_0^{(l)}(\bar{R})^T,\dots,\mathbf{m}_{\bar{R}-1}^{(l)}(\bar{R})^T)^T$, with sub-vectors $\mathbf{m}_r^{(l)}(\bar{R})=(\mathbf{m}_r^{1,(l)}(\bar{R})^T,\dots,\mathbf{m}_r^{\bar{R}-r,(l)}(\bar{R})^T)^T$, for $0\leq r\leq\bar{R}-1$. Then, Eq. (9) yields a system similar to (7), and similar arguments than those ones in Algorithm 1M (Part 1) apply for obtaining Algorithm 1M (Part 2) for computing $\mathbf{m}^{(l)}(\bar{R})$. This procedure works efficiently by computing moments of order p from previously computed moments of order $(p-1)$, with $\mathbf{m}^{(0)}(\bar{R})=\mathbf{g}(\bar{R};0)$ obtained from Algorithm 1M (Part 1), until desired value $p=l$ is reached. Once moments $m_{\mathbf{x}}^{(l)}(\bar{R})$ are in hand, the desired lth order moment $m_{\mathbf{x}}^{(l)}$ of the length of the outbreak is given by Eq. (5).

By applying Order A, Algorithm 1M can be implemented once the infinitesimal generator $\mathbf{Q}(N)$ has been iteratively constructed (Appendix B). However, the computational performance of this scheme can be improved by working in a scalar manner with Order B instead. In particular, given a state $\mathbf{x}=\{(a_1,\dots,a_i),(b_1,\dots,b_r)\}\in L(r;i)$, its corresponding Laplace-Stieltjes

transform can be written as $\phi_{\mathbf{x}}(\bar{R};z)=\phi^{(a_1,\ldots,a_i)}_{(b_1,\ldots,b_r)}(\bar{R};z)$. Then, Eq. (6) is

$$\phi^{(a_1,\ldots,a_i)}_{(b_1,\ldots,b_r)}(\bar{R};z)=\sum_{\substack{j\in\{1,\ldots,N\}\\ j\notin\{a_1,\ldots,a_i\}\\ j\notin\{b_1,\ldots,b_r\}}}\frac{\lambda_j+\sum_{i'=1}^{i}\beta_{a_{i'}j}}{z+q^{(a_1,\ldots,a_i)}_{(b_1,\ldots,b_r)}}\phi^{(a_1,\ldots,j,\ldots,a_i)}_{(b_1,\ldots,b_r)}(\bar{R};z)+\sum_{i'=1}^{i}\frac{\gamma_{a_{i'}}}{z+q^{(a_1,\ldots,a_i)}_{(b_1,\ldots,b_r)}}\phi^{(a_1,\ldots,a_{i'-1},a_{i'+1},\ldots,a_i)}_{(b_1,\ldots,a_{i'},\ldots,b_r)}(\bar{R};z). \tag{10}$$

Eq. (10) permits to obtain transforms corresponding to initial states $\mathbf{x}=\{(a_1,\ldots,a_i),(b_1,\ldots,b_r)\}\in L(r;i)$, which can be stored in vectors $\mathbf{g}^i_r(\bar{R};z)$ in a similar way to (8), from transforms corresponding to initial states $\mathbf{y}\in L(r;i+1)$ and $\mathbf{z}\in L(r+1;i-1)$. Then, by considering known values $\phi^{()}_{(b_1,\ldots,b_{\bar{R}})}(\bar{R};z)=1$ for any $(b_1,\ldots,b_{\bar{R}})$, $\phi^{()}_{(b_1,\ldots,b_{\bar{R}'})}(\bar{R};z)=0$ for any $(b_1,\ldots,b_{\bar{R}'})$ and $\bar{R}'\neq\bar{R}$, and $\phi^{(a_1,\ldots,a_i)}_{(b_1,\ldots,b_r)}(\bar{R};z)=0$ for any $\{(a_1,\ldots,a_i),(b_1,\ldots,b_r)\}$ with $i+r>\bar{R}$, Eq. (10) is directly implemented in Algorithm 1S (Part 1), given in Appendix C, for obtaining the desired Laplace-Stieltjes transforms. We point out that Algorithm 1S (Part 1) works in a scalar way by directly applying Eq. (10), and its practical implementation is possible by making use of Eq. (4) for localising the transform within $\mathbf{g}^i_r(\bar{R};z)$ corresponding to each state $\mathbf{x}\in L(r;i)$. Finally, by differentiating Eq. (10) we have that $m^{(l)}_{\mathbf{x}}(\bar{R})=m^{(a_1,\ldots,a_i),(l)}_{(b_1,\ldots,b_r)}(\bar{R})$ equals

$$m^{(l)}_{\mathbf{x}}(\bar{R})=\sum_{\substack{j\in\{1,\ldots,N\}\\ j\notin\{a_1,\ldots,a_i\}\\ j\notin\{b_1,\ldots,b_r\}}}\frac{\lambda_j+\sum_{i'=1}^{i}\beta_{a_{i'}j}}{q^{(a_1,\ldots,a_i)}_{(b_1,\ldots,b_r)}}m^{(a_1,\ldots,j,\ldots,a_i),(l)}_{(b_1,\ldots,b_r)}(\bar{R})+\sum_{i'=1}^{i}\frac{\gamma_{a_{i'}}}{q^{(a_1,\ldots,a_i)}_{(b_1,\ldots,b_r)}}\times m^{(a_1,\ldots,a_{i'-1},a_{i'+1},\ldots,a_i),(l)}_{(b_1,\ldots,a_{i'},\ldots,b_r)}(\bar{R})+\frac{l}{q^{(a_1,\ldots,a_i)}_{(b_1,\ldots,b_r)}}m^{(a_1,\ldots,a_i),(l-1)}_{(b_1,\ldots,b_r)}(\bar{R}), \tag{11}$$

so that Algorithm 1S (Part 2) is constructed for the computation of the restricted moments in a scalar way; see Section 5 and Appendix C for a discussion about the convenience of using Algorithm 1M or 1S.

Finally, we point out here that if $\mathbb{P}(R_{\mathbf{x}}=\bar{R})=0$, our algorithms in Appendix C report $\phi_{\mathbf{x}}(\bar{R};z)=m^{(l)}_{\mathbf{x}}(\bar{R})=0$, since $\mathbb{P}(T_{\mathbf{x}}(\bar{R})<\infty)=0$. This is related to the fact that, for certain values of parameters λ_i, γ_i and β_{ij}, some individuals may not be reached by the epidemic for certain initial states of the outbreak. In the particular case $\lambda_i>0$ for all $i\in\{1,\ldots,N\}$, $\mathbb{P}(R_{\mathbf{x}}=\bar{R})>0$ for all $\bar{R}\in\{1,\ldots,N\}$.

3.2 Maximum number of individuals simultaneously infected during an outbreak

We focus in this section on the analysis of random variables

$$I_{\mathbf{x}}^{max} = \text{“}\textit{Maximum number of individuals simultaneously infected during the outbreak, given that the current state of } \mathcal{X} \textit{ is } \mathbf{x}\text{”},$$

for states $\mathbf{x} \in \mathcal{C}$. In order to study these random variables we define the auxiliary ones

$$T_{\mathbf{x}}^{I} = \text{“}\textit{Time to reach, for the first time, exactly } I \textit{ number of individuals simultaneously infected during the outbreak, given that the current state of } \mathcal{X} \textit{ is } \mathbf{x}\text{”},$$

for states $\mathbf{x} \in \mathcal{C}$ and any given value $I \geq \#I(\mathbf{x})$, with $T_{\mathbf{x}}^{I}$ trivially 0 if $\#I(\mathbf{x}) = I$. These random variables are defective, since the outbreak can finalise without ever reaching I individuals simultaneously infected, so that $T_{\mathbf{x}}^{I} = \infty$. If we work similarly to Subsection 3.1 with Laplace-Stieltjes transforms

$$\varphi_{\mathbf{x}}(I;z) = E\left[e^{-zT_{\mathbf{x}}^{I}} 1_{\{T_{\mathbf{x}}^{I}<\infty\}}\right], \quad \Re(z) \geq 0,$$

the probability mass function of the *peak of infection*, $I_{\mathbf{x}}^{max}$, can be computed in terms of $\mathbb{P}(I_{\mathbf{x}}^{max} \geq I) = \varphi_{\mathbf{x}}(I;0)$. Moreover, the restricted lth order moments

$$n_{\mathbf{x}}^{(l)}(I) = E\left[\left(T_{\mathbf{x}}^{I}\right)^{l} 1_{\{T_{\mathbf{x}}^{I}<\infty\}}\right] = \left.\frac{d^l}{dz^l}\varphi_{\mathbf{x}}(I;z)\right|_{z=0}, \quad l \geq 1, \quad \mathbf{x} \in \mathcal{C},$$

allow us to analyse the speed at which this peak of infection is reached. Restricted Laplace-Stieltjes transforms and moments of $T_{\mathbf{x}}^{I}$ can be analysed by studying the auxiliary Markovian process $\mathcal{X}^I$ defined over $\mathcal{S}^I = \mathcal{C}^I \cup \{\hat{I}\} \cup \{\hat{R}\} \cup \mathcal{C}_0$, with

$$\mathcal{C}^I = \{\mathbf{x} \in \mathcal{C} : 1 \leq \#I(\mathbf{x}) < I,\ \#R(\mathbf{x}) \leq N - I\} = \bigcup_{r=0}^{N-I} L^I(r),$$

$$L^I(r) = \bigcup_{i=1}^{I-1} L(r;i), \quad 0 \leq r \leq N - I.$$

The absorbing macro-state $\hat{I}$ represents the existence of, at least, I individuals simultaneously infected in the original process, and it is formed by lumping every original state $\mathbf{x} \in L(r;i)$ with $0 \leq r \leq N - I$, $i \geq I$. The absorbing macro-state $\hat{R}$ represents the existence of, at least, $N - I + 1$ recovered individuals in process $\mathcal{X}$, and implies that the number I of simultaneously infected individuals can not be reached. The class $\mathcal{C}_0 = \cup_{r=0}^{N} L(r;0)$ represents the end of the outbreak without entering neither into absorbing states $\hat{I}$ or $\hat{R}$. Transitions among states within $\mathcal{C}^I$ are maintained from the process $\mathcal{X}$,

transitions from states in $\mathcal{C}^I$ towards $\{\mathbf{x} \in \mathcal{S} : \ \#I(\mathbf{x}) \geq I\}$ in process $\mathcal{X}$ are towards macro-state $\hat{I}$ in process $\mathcal{X}^I$, and transitions from states in $\mathcal{C}^I$ towards $\{\mathbf{x} \in \mathcal{S} : \ \#R(\mathbf{x}) \geq N - I + 1, \ \#I(\mathbf{x}) \geq 1\}$ in process $\mathcal{X}$ are towards macro-state $\hat{R}$ in process $\mathcal{X}^I$.

Similarly to Subsection 3.1, the restricted Laplace-Stieltjes transforms and moments of $T_{\mathbf{x}}^I$ are derived by a first-step argument. In particular, we have

$$\varphi_{\mathbf{x}}(I;z) = \sum_{j \in S(\mathbf{x})} \frac{\lambda_j + \sum\limits_{k \in I(\mathbf{x})} \beta_{kj}}{z + q_{\mathbf{x}}} \varphi_{I_j(\mathbf{x})}(I;z) + \sum_{k \in I(\mathbf{x})} \frac{\gamma_k}{z + q_{\mathbf{x}}} \varphi_{R_k(\mathbf{x})}(I;z), \tag{12}$$

for $\mathbf{x} \in \mathcal{C}^I$, where $I_j(\mathbf{x}) = \hat{I}$ if $\mathbf{x} \in L(r; I-1)$ and $j \in S(\mathbf{x})$. In a similar way, $R_j(\mathbf{x}) = \hat{R}$ if $\mathbf{x} \in L^I(N-I)$ and $j \in I(\mathbf{x})$. Boundary conditions for Eq. (12) are given by $\varphi_{\hat{I}}(I;z) = 1$, $\varphi_{\hat{R}}(I;z) = 0$, and $\varphi_{\mathbf{x}}(I;z) = 0$, $\mathbf{x} \in \mathcal{C}_0$. Eq. (12) can be written in matrix form similarly to (7), where matrices $\mathbf{A}_{r,r'}^{i,i'}(z)$ defined in Subsection 3.1 are involved again. Then, Algorithm 2M (Appendix C) can be constructed in a similar manner than Algorithm 1M, so that recursive schemes for obtaining the restricted Laplace-Stieltjes transforms $\varphi_{\mathbf{x}}(I;z)$ (stored in a macro-vector $\mathbf{h}(I;z)$) and lth order moments $n_{\mathbf{x}}^{(l)}(I)$ (by convenient differentiation of Eq. (12). Stored in a macro-vector $\mathbf{n}^{(l)}(I)$) of $T_{\mathbf{x}}^I$ are obtained. Finally, a scalar version of Algorithm 2M, Algorithm 2S (Appendix C), can be constructed by means of application of Order B in a similar manner than in Subsection 3.1. Similarly to last comments in Subsection 3.2, our algorithms report $\varphi_{\mathbf{x}}(I;z) = n_{\mathbf{x}}^{(l)}(I) = 0$ if $\mathbb{P}(I_{\mathbf{x}}^{max} \geq I) = \mathbb{P}(T_{\mathbf{x}}^I < \infty) = 0$; in the particular case $\lambda_i > 0$ for all $i \in \{1, \ldots, N\}$, $\mathbb{P}(I_{\mathbf{x}}^{max} \geq I) > 0$ for all $I \in \{\#I(\mathbf{x}), \ldots, N\}$.

3.3 Individual fate during an outbreak

In this section, we focus on a particular marked individual (without any loss of generality, the Nth individual) within the population. Our interest is in analysing the fate of this individual regarding the spread of the epidemic during the outbreak. In particular, it is clear that individual N may:

Fate A not suffer the infection during the outbreak;
Fate B suffer the infection during the outbreak, due to an external infection;
Fate C suffer the infection during the outbreak, due to an infectious contact with an infected individual within the network.

Our aim is to analyse the probability of each of these events, as well as the times until their occurrences. To that end, we define the random variables

$T_{\mathbf{x}}^B$ = *"Time until individual N is infected by an external source during the outbreak, given that the current state of $\mathcal{X}$ is $\mathbf{x}$"*,

$T_{\mathbf{x}}^C$ = *"Time until individual N is infected due to an infectious within-network contact during the outbreak, given that the current state of $\mathcal{X}$ is $\mathbf{x}$"*,

for any state $\mathbf{x} \in \mathcal{C}$, with $N \in S(\mathbf{x})$. We note here that events A, B and C are disjoint, and that random variables $T_{\mathbf{x}}^B$ and $T_{\mathbf{x}}^C$ are defective so that

$$T_{\mathbf{x}}^B < \infty \Leftrightarrow \text{B}, \quad T_{\mathbf{x}}^C < \infty \Leftrightarrow \text{C}, \quad \left(T_{\mathbf{x}}^B = \infty \wedge T_{\mathbf{x}}^C = \infty\right) \Leftrightarrow \text{A}.$$

If we define the restricted Laplace-Stieltjes transforms

$$\xi_{\mathbf{x}}^W(z) = E\left[e^{-zT_{\mathbf{x}}^W} 1_{\{T_{\mathbf{x}}^W < \infty\}}\right], \quad W \in \{B, C\},$$

for $\Re(z) \geq 0$, we have that $\xi_{\mathbf{x}}^W(0) = \mathbb{P}(W)$ for $W \in \{B, C\}$, while $\mathbb{P}(A) = 1 - \mathbb{P}(B) - \mathbb{P}(C)$. Fate A can also be analysed in terms of the time until B or C occurs (time until infection of individual N, regardless of the infection's cause), $T_{\mathbf{x}}^{B\vee C} = min\{T_{\mathbf{x}}^B, T_{\mathbf{x}}^C\}$, where

$$\xi_{\mathbf{x}}^{B\vee C}(z) = E\left[e^{-zT_{\mathbf{x}}^{B\vee C}} 1_{\{T_{\mathbf{x}}^{B\vee C} < \infty\}}\right] \; = \; \xi_{\mathbf{x}}^B(z) + \xi_{\mathbf{x}}^C(z),$$

so that $\mathbb{P}(N \textit{ suffering an infection during the outbreak}) = \xi_{\mathbf{x}}^{B\vee C}(0)$, and $\mathbb{P}(A) = 1 - \xi_{\mathbf{x}}^{B\vee C}(0)$. The analysis of $\xi_{\mathbf{x}}^{B\vee C}(z)$ permits to compute statistical measures of the time until the infection of individual N:

$$m_{\mathbf{x}}^{B\vee C,(l)} = E\left[\left(T_{\mathbf{x}}^{B\vee C}\right)^l 1_{\{T_{\mathbf{x}}^{B\vee C} < \infty\}}\right] \; = \; \frac{d^l}{dz^l}\xi_{\mathbf{x}}^{B\vee C}(z)\Big|_{z=0}, \quad l \geq 1.$$

Laplace-Stieltjes transforms $\xi_{\mathbf{x}}^B(z)$ and $\xi_{\mathbf{x}}^C(z)$ can be computed by means of

$$\begin{aligned}\xi_{\mathbf{x}}^W(z) = \sum_{j \in S(\mathbf{x}),\ j \neq N} \frac{\lambda_j + \sum\limits_{k \in I(\mathbf{x})} \beta_{kj}}{z + q_{\mathbf{x}}} \xi_{I_j(\mathbf{x})}^W(z) + \delta_{W,C} \frac{\sum\limits_{k \in I(\mathbf{x})} \beta_{kN}}{z + q_{\mathbf{x}}} \\ + \delta_{W,B} \frac{\lambda_N}{z + q_{\mathbf{x}}} + \sum_{k \in I(\mathbf{x})} \frac{\gamma_k}{z + q_{\mathbf{x}}} \xi_{R_k(\mathbf{x})}^W(z),\end{aligned} \tag{13}$$

for $W \in \{B, C\}$ and for states $\mathbf{x} \in \hat{\mathcal{C}}$, with

$$\hat{\mathcal{C}} = \{\mathbf{x} \in \mathcal{S} :\ 1 \leq \#I(\mathbf{x}) \leq N - 1,\ N \in S(\mathbf{x})\} \; = \; \bigcup_{r=0}^{N-2} \hat{L}^{(N)}(r).$$

We reintroduce here the superscript N in the notation so that

$$\hat{L}^{(N)}(r) = \{\mathbf{x} \in \hat{\mathcal{C}} :\ \#R(\mathbf{x}) = r\} \; = \; \bigcup_{i=1}^{N-r-1} \hat{L}^{(N)}(r; i), \quad 0 \leq r \leq N - 2,$$

$$\hat{L}^{(N)}(r; i) = \{\mathbf{x} \in \hat{L}^{(N)}(r) :\ \#I(\mathbf{x}) = i\}, \quad 1 \leq i \leq N - r - 1.$$

Then, $\hat{L}^{(N)}(r; i)$ can be reexpressed in terms of the original sub-level for a population with $N - 1$ individuals, $L^{(N-1)}(r; i)$, as

$$\hat{L}^{(N)}(r; i) = L^{(N-1)}(r; i) \times \{S\}, \quad 0 \leq r \leq N - 2, \quad 1 \leq i \leq N - r - 1 \tag{14}$$

Expression (14) follows from the fact that individual N is known to be susceptible in any state $\mathbf{x} \in \hat{\mathcal{C}}$, so that the possible different configurations of $\mathbf{x}$ consist of the possible states of individuals $\{1, \ldots, N-1\}$.

If we store restricted transforms $\xi_{\mathbf{x}}^{W}(z)$ in a macro-vector $\mathbf{f}^{W}(z)$, for $W \in \{B, C\}$, structured as $\mathbf{f}^{W}(z) = (\mathbf{f}_0^{W}(z)^T, \mathbf{f}_1^{W}(z)^T, \ldots, \mathbf{f}_{N-2}^{W}(z)^T)^T$, with $\mathbf{f}_r^{W}(z) = (\mathbf{f}_r^{1,W}(z)^T, \mathbf{f}_r^{2,W}(z)^T, \ldots, \mathbf{f}_r^{N-r-1,W}(z)^T)^T$, for $0 \leq r \leq N-2$, then we can express (13) in matrix form as

$$\mathbf{f}^{W}(z) = \hat{\mathbf{A}}(z)\mathbf{f}^{W}(z) + \mathbf{c}^{W}(z),$$

where matrix $\hat{\mathbf{A}}(z)$ has the same bidiagonal-by-blocks structure than matrix $\mathbf{A}(N-1; z)$ in (7) but with sub-matrices $\mathbf{A}_{r,r'}^{i,i'}(z)$ replaced by $\hat{\mathbf{A}}_{r,r'}^{i,i'}(z)$. According to Eqs. (13)-(14), each sub-matrix $\hat{\mathbf{A}}_{r,r'}^{i,i'}(z)$ is obtained by dividing each $\mathbf{x}$th row of matrix $\mathbf{Q}_{r,r'}^{i,i'}(N-1)$ by $z+q_{\mathbf{x}}$, and vector $\mathbf{c}^{W}(z)$ is given as $\mathbf{c}^{W}(z) = (\mathbf{c}_0^{W}(z)^T, \mathbf{c}_1^{W}(z)^T, \ldots, \mathbf{c}_{N-2}^{W}(z)^T)^T$, with $\mathbf{c}_r^{W}(z) = (\mathbf{c}_r^{1,W}(z)^T, \mathbf{c}_r^{2,W}(z)^T, \ldots, \mathbf{c}_r^{N-r-1,W}(z)^T)^T$, for $0 \leq r \leq N-2$ and $W \in \{B, C\}$. Finally, $\mathbf{c}_r^{i,W}(z)$ for $W = B$ and $W = C$ is obtained by dividing each $\mathbf{x}$th row of $\mathbf{U}_r^{i}(N-1)\mathbf{e}_{J^{(N-1)}(r;i)}$ and $\lambda_N \mathbf{e}_{J^{(N-1)}(r;i)}$, respectively, by $z + q_{\mathbf{x}}$, where $\mathbf{U}_r^{i}(N-1)$ is a particular sub-matrix obtained during the iterative computation of the infinitesimal generator $\mathbf{Q}(N)$ in Appendix B.

The structure of $\hat{\mathbf{A}}(z)$ means that a particular adaptation of Algorithm 1M (not reported here) permits to compute, in an iterative manner, restricted transforms $\xi_{\mathbf{x}}^{W}(z)$ for $W \in \{B, C\}$. In the same manner, successive differentiation in (13) yields the analogous of Algorithm 1M (Part 2), for computing the lth order restricted moments $m_{\mathbf{x}}^{W,(l)} = E\left[\left(T_{\mathbf{x}}^{W}\right)^l 1_{\{T_{\mathbf{x}}^{W} < \infty\}}\right]$, for $W \in \{B, C\}$. Finally, the lth order restricted moment of the time until infection of individual N is $m_{\mathbf{x}}^{B \vee C,(l)} = m_{\mathbf{x}}^{B,(l)} + m_{\mathbf{x}}^{C,(l)}$. We note here that an analogous algorithm than Algorithm 1S for obtaining previous quantities in a scalar way following Order B can be obtained, in a similar manner than in Subsections 3.1 and 3.2. We point out that our procedures in Appendix C report values $\xi_{\mathbf{x}}^{B \vee C}(z) = m_{\mathbf{x}}^{B \vee C,(l)} = 0$ if $\mathbb{P}(B \vee C) = \mathbb{P}(T^{B \vee C} < \infty) = 0$, and that $\mathbb{P}(B \vee C) > 0$ if $\lambda_i > 0$ for all $i \in \{1, \ldots, N\}$.

3.4 Exact reproduction number of a given individual

The basic reproduction number, R_0, is the most widely used measure of disease spread in epidemiological models both from the stochastic and deterministic point of view. It is defined, for well-mixed homogeneous populations, as the mean number of infections directly caused by a typical individual during his infectious period in a completely susceptible population. This permits to interpret R_0 in many models in terms of threshold values for analysing the epidemic prevalence in the long-term. In the stochastic framework, it has been recently shown in [3,34] the convenience of replacing this descriptor by its *exact* counterpart when dealing with finite populations. The exact reproduction number,

$R_{\mathbf{x}}^{exact}$, is defined in [3] as the random variable denoting the number of individuals directly infected by a given one during his infectious period given the current state of the process $\mathbf{x}$. This random variable, for $\mathbf{x}$ representing an individual starting the infection within a fully susceptible population, was previously introduced and analysed in [34], for the SIS and SIR epidemic models in finite homogeneous populations, and for recovery times distributed as exponential, two-phase gamma and constant distributions. Then, the infectiousness of a particular individual can be measured in terms of a random variable instead of an average quantity, allowing us to consider different possible initial states $\mathbf{x}$. $R_{\mathbf{x}}^{exact}$ can be seen as an extension of the basic reproduction number, since $E[R_{\mathbf{x}}^{exact}] = R_0$ when the considered initial state $\mathbf{x}$ represents that the analysed infected individual initiates the epidemic throughout a completely susceptible population.

It is not immediate how to define $R_{\mathbf{x}}^{exact}$ for the case of an heterogeneous population, where the selected particular individual directly affects the exact reproduction number under study. In [13], an individual-based version of the exact reproduction number for heterogeneous populations is proposed, and this version is the one that we analyse here. In particular, we define the exact reproduction number of each individual $i \in \{1, \ldots, N\}$ as the random variable

$$R_{\mathbf{x}}^{exact}(i) = \text{“}\textit{Number of infections directly caused by the individual } i \textit{ during his infectious period, given that the current state of } \mathcal{X} \textit{ is } \mathbf{x} \in \mathcal{C}\text{”},$$

for $i \in I(\mathbf{x})$, so that $R_{\mathbf{x}}^{exact}(i)$ is an individual measure of infectiousness, and has support $\{0, \ldots, \#S(\mathbf{x})\}$.

From now on, we focus on individual N without any loss of generality, and denote $R_{\mathbf{x}}^{exact}(N) = R_{\mathbf{x}}^{exact}$. The analysis of $R_{\mathbf{x}}^{exact}$ for the state $\mathbf{x} = (S, \ldots, S, I)$ is of particular interest since it represents the number of infections caused by individual N during his infectious period when the rest of individuals are initially susceptible.

We analyse the probability mass function of $R_{\mathbf{x}}^{exact}$ by means of its probability generating function $\mu_{\mathbf{x}}(s) = E[s^{R_{\mathbf{x}}^{exact}}]$, with $|s| \leq 1$, which verifies the equation

$$\begin{aligned}\mu_{\mathbf{x}}(s) = \sum_{j \in S(\mathbf{x})} & \frac{\lambda_j + s\beta_{Nj} + \sum\limits_{k \in I(\mathbf{x}), k \neq N} \beta_{kj}}{q_{\mathbf{x}}} \mu_{I_j(\mathbf{x})}(s) \\ & + \sum_{k \in I(\mathbf{x}), k \neq N} \frac{\gamma_k}{q_{\mathbf{x}}} \mu_{R_k(\mathbf{x})}(s) + \frac{\gamma_N}{q_{\mathbf{x}}}, \quad |s| \leq 1,\end{aligned} \tag{15}$$

with boundary conditions $\mu_{\mathbf{x}}(s) = 1$ if $\#I(\mathbf{x}) + \#R(\mathbf{x}) = N$, $N \in I(\mathbf{x})$. In a matrix form, we consider Order A and store the quantities $\mu_{\mathbf{x}}(s)$ in vectors $\boldsymbol{\mu}(s) = (\boldsymbol{\mu}_0(s)^T, \boldsymbol{\mu}_1(s)^T, \ldots, \boldsymbol{\mu}_{N-1}(s)^T)^T$, with $\boldsymbol{\mu}_r(s) = (\boldsymbol{\mu}_r^1(s)^T, \boldsymbol{\mu}_r^2(s)^T, \ldots, \boldsymbol{\mu}_r^{N-r}(s)^T)^T$, $0 \leq r \leq N-1$, where sub-vector $\boldsymbol{\mu}_r^i(s)$ contains quantities $\mu_{\mathbf{x}}(s)$ for states $\mathbf{x} \in \bar{L}^{(N)}(r; i) = \{\mathbf{x} \in \mathcal{C} : \ \#I(\mathbf{x}) = i, \ \#R(\mathbf{x}) = r, \ N \in I(\mathbf{x})\} = L^{(N-1)}(r; i-1) \times \{I\}$, so that $\#\bar{L}^{(N)}(r; i) = J^{(N-1)}(r; i-1)$. Boundary conditions mean that

$\boldsymbol{\mu}_r^{N-r}(s) = \mathbf{e}_{J^{(N-1)}(r;N-r-1)}$ for all $0 \leq r \leq N-1$, and permit to recursively solve the system in (15). This can be written as

$$\begin{pmatrix} \boldsymbol{\mu}_0(s) \\ \boldsymbol{\mu}_1(s) \\ \vdots \\ \boldsymbol{\mu}_{N-2}(s) \end{pmatrix} = \begin{pmatrix} \bar{\mathbf{A}}_{0,0} & \bar{\mathbf{A}}_{0,1} & \dots & \mathbf{0} \\ \mathbf{0} & \bar{\mathbf{A}}_{1,1} & \dots & \mathbf{0} \\ \mathbf{0} & \mathbf{0} & \dots & \mathbf{0} \\ \vdots & \vdots & \ddots & \vdots \\ \mathbf{0} & \mathbf{0} & \dots & \bar{\mathbf{A}}_{N-2,N-1} \end{pmatrix} \begin{pmatrix} \boldsymbol{\mu}_0(s) \\ \boldsymbol{\mu}_1(s) \\ \vdots \\ \boldsymbol{\mu}_{N-1}(s) \end{pmatrix} + \begin{pmatrix} \bar{\mathbf{c}}_0 \\ \bar{\mathbf{c}}_1 \\ \vdots \\ \bar{\mathbf{c}}_{N-2} \end{pmatrix}, \tag{16}$$

where matrices $\bar{\mathbf{A}}_{r,r'}$ are given as

$$\bar{\mathbf{A}}_{r,r} = \begin{pmatrix} \mathbf{0} & \bar{\mathbf{A}}_{r,r}^{1,2} & \dots & \mathbf{0} \\ & +s\mathbf{Q}_{r,r}^{0,1,\lambda}(N-1, \underline{\boldsymbol{\beta}}_{N\cdot}^T) & & \\ \mathbf{0} & \mathbf{0} & \dots & \mathbf{0} \\ \mathbf{0} & \mathbf{0} & \dots & \mathbf{0} \\ \vdots & \vdots & \ddots & \vdots \\ \mathbf{0} & \mathbf{0} & \dots & \bar{\mathbf{A}}_{r,r}^{N-r-1,N-r} \\ & & & +s\mathbf{Q}_{r,r}^{N-r-2,N-r-1,\lambda}(N-1, \underline{\boldsymbol{\beta}}_{N\cdot}^T) \\ \mathbf{0} & \mathbf{0} & \dots & \mathbf{0} \end{pmatrix},$$

for $0 \leq r \leq N-2$, and

$$\bar{\mathbf{A}}_{r,r+1} = \begin{pmatrix} \mathbf{0} & \mathbf{0} & \mathbf{0} \dots & \mathbf{0} & \mathbf{0} \\ \bar{\mathbf{A}}_{r,r+1}^{2,1} & \mathbf{0} & \mathbf{0} \dots & \mathbf{0} & \mathbf{0} \\ \mathbf{0} & \bar{\mathbf{A}}_{r,r+1}^{3,2} & \mathbf{0} \dots & \mathbf{0} & \mathbf{0} \\ \vdots & \vdots & \vdots \ddots & \vdots & \vdots \\ \mathbf{0} & \mathbf{0} & \mathbf{0} \dots & \bar{\mathbf{A}}_{r,r+1}^{N-r-1,N-r-2} & \mathbf{0} \\ \mathbf{0} & \mathbf{0} & \mathbf{0} \dots & \mathbf{0} & \bar{\mathbf{A}}_{r,r+1}^{N-r,N-r-1} \end{pmatrix},$$

for $0 \leq r \leq N-2$, and where sub-matrices $\bar{\mathbf{A}}_{r,r'}^{i,i'}$ are obtained by dividing each $\mathbf{x}$th row of matrices $\mathbf{Q}_{r,r'}^{i-1,i'-1}(N-1)$ by $q_{\mathbf{x}}$. Matrices $\mathbf{Q}_{r,r}^{i,i+1,\lambda}(N-1, \underline{\boldsymbol{\beta}}_{N\cdot}^T)$ are defined in the iterative construction of the infinitesimal generator $\mathbf{Q}(N)$ in Appendix B. Finally, we have $\bar{\mathbf{c}}_r = ((\bar{\mathbf{c}}_r^1)^T, (\bar{\mathbf{c}}_r^2)^T, \dots, (\bar{\mathbf{c}}_r^{N-r-1})^T, (\bar{\mathbf{c}}_r^{N-r})^T)^T$, with $(\bar{\mathbf{c}}_r^i)_{\mathbf{x}} = \frac{\gamma_N}{q_{\mathbf{x}}}$, for $1 \leq i \leq N-r$, $0 \leq r \leq N-2$. Algorithm 3M (Part 1) iteratively solves (16) (Appendix C).

Once the probability generating functions are in hand, the lth order factorial moment of $R_{\mathbf{x}}^{exact}$ and its probability mass function are computed as

$$E\left[R_{\mathbf{x}}^{exact}(R_{\mathbf{x}}^{exact}-1)\dots(R_{\mathbf{x}}^{exact}-l+1)\right] = \left.\frac{d^l}{ds^l}\mu_{\mathbf{x}}(s)\right|_{s=1}, \quad l \geq 1,$$

$$\mathbb{P}(R_{\mathbf{x}}^{exact} = k) = \left.\frac{1}{k!}\frac{d^k}{ds^k}\mu_{\mathbf{x}}(s)\right|_{s=0}, \quad 0 \leq k \leq \#S(\mathbf{x}),$$

computations that can be carried out in an algorithmic manner (see Algorithm 3M (Part 2) in Appendix C for the algorithmic computation of factorial moments). Moreover, a scalar analogous version of Algorithm 3M, Algorithm 3S which is omitted here, can be constructed by means of usage of Order B, and by similar arguments than those ones followed in previous subsections.

4 Numerical Results

For purely illustrative purposes, we analyse here a simple model for the spread of *Methicillin-resistant Staphylococcus Aureus* (MRSA) among the patients within an intensive care unit (ICU). MRSA is a particular group of *S. aureus* strains which are resistant to beta-lactam antibiotics, and represent a major challenge especially in particular small populations settings such as ICUs [4] and prisons [20]. Different attempts have been made during the last years for analysing epidemiological data [11,14] and developing mathematical models [4,5] regarding this disease, in order to understand its spread dynamics and to quantitatively analyse the implementation of control strategies.

In [4], a Markovian approach is followed for studying the spread of MRSA within an ICU, and stochastic descriptors, such as the exact reproduction number, are analysed. Main assumptions in [4] amount to the consideration of two well-mixed homogeneous populations within the ICU, patients and healthcare workers (HCWs), and the assumption that once a particular patient is recovered he is immediately replaced by a new one. However, the consideration of well-mixed populations does not permit to study the implementation of control strategies, such as isolation measures or room management, that intrinsically introduce heterogeneities among the individuals of the population. We propose to analyse these strategies following our approach, but by considering HCWs as vectors for MRSA, so that they are only implicitly considered in our model by means of the infection rates β_{ij} [11]. Our main simplifying assumption here is that no discharge of patients is considered during the outbreak, which in our numerical results lasts for $\sim 11-16$ *days*. This restrictive assumption allows us to directly illustrate the analysis developed in Sections 2-3, and to evaluate the impact that the dynamical discharge and admission of patients may have in our descriptors. This impact is addressed, by means of stochastic simulations and for a particular descriptor (individual fate), in Section 5, where discharge and admission of patients is incorporated.

We consider an ICU with 9 patients, which is the mean occupancy of beds within the ICU considered in a similar process in [14]. We point out here that, as reported in [41], an ICU should accommodate between 8 and 12 beds. From [11, Table 2], where authors apply structured and standard hidden Markov models for estimating the transmission rate of MRSA among patients within a hospital, we consider a general transmission rate for a well-mixed population of patients equal to $\hat{\beta} = 0.329\ days^{-1}$. Since we are applying mass-action kinetics in Eq. (1), $\beta = \hat{\beta}/9$ represents in our model the rate at which each susceptible patient is infected by each infected patient under homogeneous

mixing assumptions. We introduce heterogeneity in our model in order to analyse two different control strategies commonly implemented to avoid outbreaks of MRSA: (i) a proper organisation of rooms, trying to configure the ICU in an *uncrowded* fashion when possible [41], and (ii) the isolation of the individual which is found to start an outbreak within the ICU [14]. Thus, when patient 1 initiates the outbreak (initial state $\mathbf{x} = (I, S, \ldots, S)$), we consider six possible scenarios depending on the implementation of the strategies previously mentioned. This yields scenarios IS.U, IS.C and IS.O (patient 1 is isolated, and the ICU is configured in an *uncrowded*, *crowded* or *overcrowded* fashion, respectively) and scenarios NIS.U, NIS.C and NIS.O (patient 1 is not isolated); see Figure 2. Rates in Eq. (1) are set as follows:

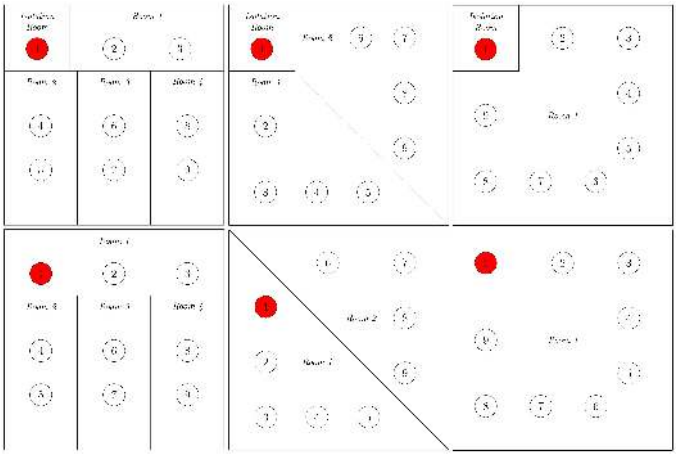

Fig. 2 ICU configuration when patient 1 is isolated (*top*) or is not isolated (*bottom*), under (from *left* to *right*) uncrowded, crowded or ovecrowded room configurations. Patient 1 (red circle) initiates the outbreak

(a) For individuals within the same room $i, j \in \mathcal{N}$, we consider $\beta_{ij} = \beta_{ji} = \beta$.
(b) For patient 1 isolated in scenarios IS.U, IS.C and IS.O, we consider $\beta_{1j} = 0.3\beta$ for all $j \in \mathcal{N}$, to represent a 70% decrease in its infectiousness due to isolation, which has been estimated in [14]. As stated in [14], isolation conditions do not only consist of placing patient 1 in a different room, but this room being specially equipped for avoiding infection transmission (handwashing policy posted at the entrance of the room, sink with gloves, soap antibacterial scrub solution and skin moisturiser available).
(c) For patients $i, j \in \mathcal{N}$ in different non-isolated rooms (e.g. patients 2 and 4 in scenario IS.U), and due to the lack of proper data, we consider for illustrative purposes $\beta_{ij} = \beta_{ji} = 0.65\beta$. This represents a medium effectiveness of room separation between cases (a) (patients within the same room) and (b) (infected patient in the isolation room).

(d) Patients suffering MRSA can have very different behaviours against the disease, so that their recovery can long from some *days* up to several *weeks* [26]. However, the majority of patients require a treatment of around $5-10$ *days* when dealing with MRSA presented in terms of skin and soft-tissue infections or regarding nasal decolonization [26, Sections I-II]. Thus, we consider a mean recovery period here of $1/\gamma = 1$ *week*.
(e) The main external source for introducing MRSA within the ICU is the admission of new patients which can carry the disease, this admission not being considered here when studying a particular outbreak. We point out that time $t = 0$ in our process may be considered as the admission time of patient 1, which was carrying MRSA. To represent other external sources of infection (such as contaminated equipment, hospital staff infected by individuals outside the ICU) we set $\lambda_i = 0.1\beta$ for all $i \in \mathcal{N}$.

In Figure 3 we display the probability mass function of the size $R_{\mathbf{x}}$ of the outbreak and the mean length of the outbreak, under each scenario, obtained from Algorithms 1S-1M. When patient 1 is isolated, it is clear that $\mathbb{P}(R_{\mathbf{x}} = 1)$ represents the probability of the patient 1 recovering before any other infection occurs, which does not depend on the room configuration. However, this probability of the infection not occurring in any other patient during the outbreak clearly depends on the isolation state of patient 1 (e.g. $\mathbb{P}(R_{\mathbf{x}} = 1) = 0.5498$ in scenario IS.U against $\mathbb{P}(R_{\mathbf{x}} = 1) = 0.3684$ in scenario NIS.U). When patient 1 is isolated, room configuration becomes important once the infection has escaped isolation room. Results in Figure 3 suggest that room configuration plays a more important role under non-isolation of patient 1. At the same time, the mean length of the outbreak takes values between 11 and 16 *days*, so that the different preventive measures considered here not only reduce the probability of avoiding the infection of any other patient (reduction up to 35%), but also the expected length of the outbreak (reduction up to 28%). Bimodal shape of the probability mass function of $R_{\mathbf{x}}$ represents a two-output situation: if the disease does not *escape* patient 1, then $R_{\mathbf{x}} = 1$. If it escapes patient 1, the potential of this epidemic within the ICU leads to a total size of the outbreak that is directly related to the *second mode* of this distribution.

Exact values computed here by means of our approach could be efficiently approximated instead by means of Gillespie simulations [16]. For example, 10^4 stochastic simulations of our process yield values of $E[T_{\mathbf{x}}]$ equal to 11.6729, 11.9862 and 12.1660 *days* for the mean length of the outbreak in scenarios IS.U, IS.C and IS.O, respectively. These values are in good correspondence with values computed in Figure 3, where slight deviations are directly related to the standard deviation of $T_{\mathbf{x}}$ under these scenarios. In particular, Algorithm 1S in Appendix C allows us to compute the standard deviation of $T_{\mathbf{x}}$, $SD[T_{\mathbf{x}}]$, which equals 12.8063, 13.0002 and 13.2812 *days* under these scenarios. These yield variation coefficients, $CV[T_{\mathbf{x}}] = SD[T_{\mathbf{x}}]/E[T_{\mathbf{x}}]$, equal to 1.0957, 1.0918 and 1.0808 for isolation scenarios, which means that variable $T_{\mathbf{x}}$ can be classified as *high-variance* by direct comparison with the exponential distribution.

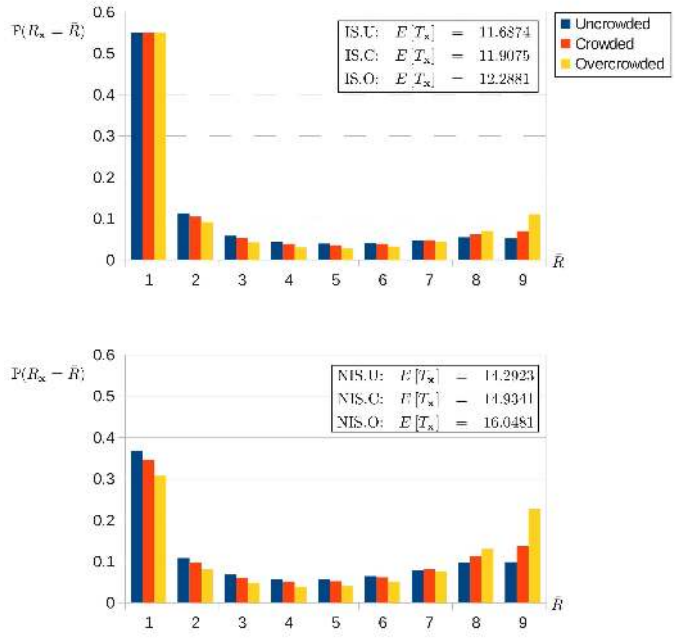

Fig. 3 Probability mass function of the size $R_{\mathbf{x}}$ of the outbreak and mean length $E[T_{\mathbf{x}}]$ (in *days*) of the outbreak for isolation (*top*) and non-isolation (*bottom*) scenarios. Patient 1 initiates the outbreak, $\mathbf{x} = (I, S, \ldots, S)$

In Figure 4 the probability mass function of the maximum number $I_{\mathbf{x}}^{max}$ of simultaneously infected individuals as well as its average are computed by means of Algorithms 2S-2M, where it is worth noting that $\mathbb{P}(I_{\mathbf{x}}^{max} = 1) = \mathbb{P}(R_{\mathbf{x}} = 1)$. In most of the cases, the bimodal distribution shown in Figure 4 represents a two-output situation related to results in Figure 3: either the peak of infection will be equal to 1 if patient 1 recovers soon enough, or it will be at some point in $\{2, \ldots, 9\}$ represented by the *second mode* if infection escapes from patient 1 to other patients within the ICU. Again, the most effective strategy is the isolation of patient 1, yielding smaller values of $E[I_{\mathbf{x}}^{max}]$ regardless of room configuration. If patient 1 is not isolated, room configuration becomes significantly more important for the peak of infection. In general, control measures can reduce the mean peak of infection $E[I_{\mathbf{x}}^{max}]$ up to a 37%.

Main insights previously obtained stress the importance of isolation of patient 1 initiating the outbreak, which is directly related to the importance of implementing proper screening policies so that this isolation can take place as soon as patient 1 is infected [40]. Room configuration then must be seen as a more general preventive strategy so that, if infection of patient 1 goes unnoticed (or if the ICU does not contain an available isolation room), uncrowded ICUs would lead to better epidemic scenarios.

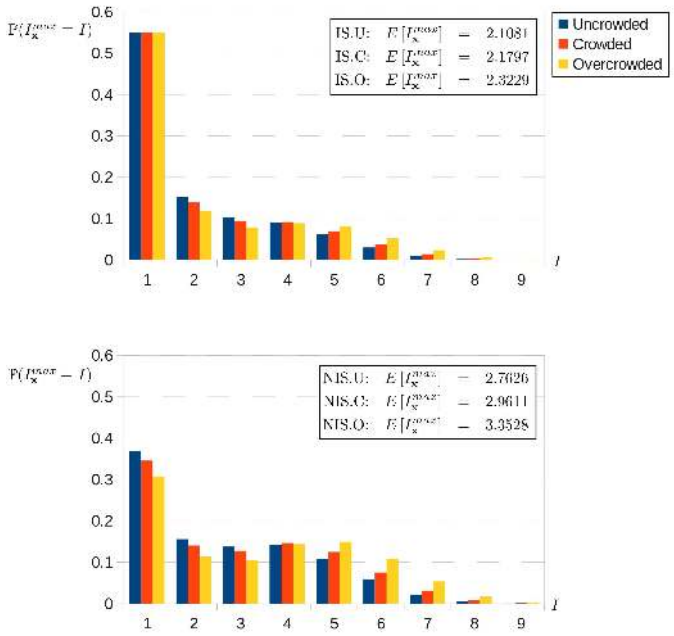

Fig. 4 Probability mass function of the maximum number $I_{\mathbf{x}}^{max}$ of patients simultaneously infected during the outbreak and its mean $E[I_{\mathbf{x}}^{max}]$ for isolation (*top*) and non-isolation (*bottom*) scenarios. Patient 1 initiates the outbreak, $\mathbf{x} = (I, S, \ldots, S)$

Figure 5 permits to clarify the speed of the spread of the epidemic among patients within the ICU, by displaying the conditioned mean times $E[T_{\mathbf{x}}^I | T_{\mathbf{x}}^I < \infty]$ to reach each possible peak $I \in \{1, \ldots, 9\}$. These times take values from 0 (for the trivial case $I = 1$) up to 10 *days* (12 *days*) under isolation (non-isolation) of patient 1. Results in Figure 5 show a stabilisation of $E[T_{\mathbf{x}}^I | T_{\mathbf{x}}^I < \infty]$ for values greater than $I = 5$, where even a slight decrease can be observed for large enough values of I (these values being reached with very low probability; see Figure 4). This represents the fact that, if a large number I of infected individuals is obtained during the outbreak, infections should have occurred *quick enough* so that recoveries did not lead to the end of the outbreak before this value I of simultaneously infected individuals is reached. For example, if we carry out 10^6 stochastic simulations of our process for scenario IS.C, mean time $E[T_{\mathbf{x}}^6 | T_{\mathbf{x}}^6 < \infty]$ to reach 6 infected individuals (conditioning on this event occurring) is 11.146773 *days* (event that occurred in 5.45% of our simulations); on the other hand, the mean time $E[T_{\mathbf{x}}^9 | T_{\mathbf{x}}^9 < \infty]$ to reach 9 infected individuals (conditioning on this event occurring) is 10.33141 *days*, but this event only occurred in 0.046% of our simulations.

Individual fate is analysed in Table 1, so that the probability of infection of each particular patient (and the expected time until this occurring) is computed for an outbreak initiated by patient 1. We point out that, under each

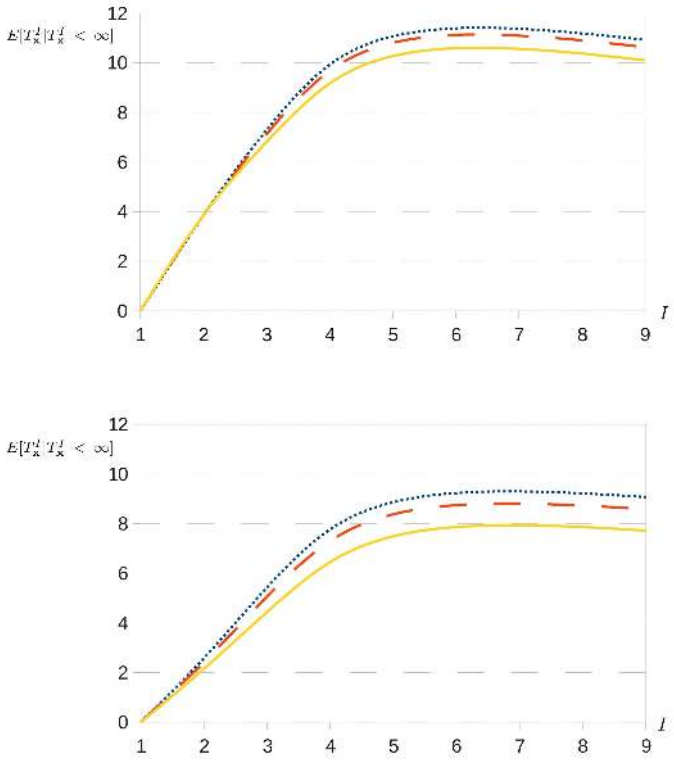

Fig. 5 Conditioned mean time $E[T_{\mathbf{x}}^I | T_{\mathbf{x}}^I < \infty]$ (in *days*) until reaching I individuals simultaneously infected during the outbreak versus I for isolation (*top*) and non-isolation (*bottom*) scenarios. Uncrowded (*dotted*), crowded (*dashed*) and overcrowded (*solid*) room configurations considered. Patient 1 initiates the outbreak, $\mathbf{x} = (I, S, \ldots, S)$

scenario, several patients behave equally with respect the epidemic started by patient 1, so that their individual fate probabilities are equal (e.g. patients $\{2, \ldots, 9\}$ in scenario IS.O). Thus, in Table 1 those individuals with identical individual behaviour against the disease are grouped together. Under any scenario, probability $\mathbb{P}(B)$ of any individual becoming infected by exterior sources of infection is always smaller than the probability $\mathbb{P}(C)$ of becoming infected due to an infectious contact, which is directly related with the considered values of λ_i, $i \in \{2, \ldots, 9\}$. Preventive strategies can increase the probability of a particular individual within the ICU avoiding the infection up to a 50% (e.g. patient 2: $\mathbb{P}(A) = 0.5132$ in scenario NIS.O against $\mathbb{P}(A) = 0.7734$ in scenario IS.U). At the same time, the conditioned expected time $E[T_{\mathbf{x}}^{B\vee C} | T_{\mathbf{x}}^{B\vee C} < \infty]$ until infection of a particular individual can also be increased from 7.32 *days* up to 10.10 *days* by implementing control measures. In scenarios NIS.U and NIS.C we have to make the distinction between the individual fate of a patient who is sharing or not his room with patient 1. It is worth noting that, for a particular individual, his condition of sharing the room with initial infected

patient 1 only produces a total increase of 0.0316 in his probability of suffering the infection (patients 2 and 6 in scenario NIS.U, similarly in scenario NIS.C), while this probability $\mathbb{P}(A)$ increases significantly more by implementing preventive measures (e.g. from 0.6110 to 0.7734 by isolating patient 1). This suggests that, even from an individual perspective, it is noticeably more efficient for an arbitrary individual the complete isolation of the patient initiating the outbreak than the simple avoidance of sharing the room with him.

Table 1 Analysis of individual fate for different patients within the ICU, and under different scenarios. Patient 1 initiates the outbreak, $\mathbf{x} = (I, S, \dots, S)$. Fates of individual i: A: no infection; B: *external* infection; C: *within-network contact* infection; $B \vee C$: infection.

Isolated	IS.U		IS.C		IS.O
Fate of Patient i	$i \in \mathcal{N}$		$i \in \mathcal{N}$		$i \in \mathcal{N}$
Probability of event A	0.7734		0.7573		0.7270
Probability of event B	0.0282		0.0277		0.0265
Probability of event C	0.1984		0.2151		0.2464
Mean restricted time to B $E[T_{\mathbf{x}}^{B} 1_{\{T_{\mathbf{x}}^{B}<\infty\}}]$	0.2285		0.2182		0.1970
Mean restricted time to C $E[T_{\mathbf{x}}^{C} 1_{\{T_{\mathbf{x}}^{C}<\infty\}}]$	2.0602		2.2205		2.4832
Mean restricted time to $B \vee C$ $E[T_{\mathbf{x}}^{B\vee C} 1_{\{T_{\mathbf{x}}^{B\vee C}<\infty\}}]$	2.2887		2.4387		2.6802
Mean conditioned time to $B \vee C$ $E[T_{\mathbf{x}}^{B\vee C} \mid \{T_{\mathbf{x}}^{B\vee C} < \infty\}]$	10.1005		10.0467		9.8192
Non-isolated	NIS.U		NIS.C		NIS.O
Fate of Patient i	$i \in \{2,3\}$	$i \in \{4,\dots,9\}$	$i \in \{2,\dots,5\}$	$i \in \{6,\dots,9\}$	$i \in \mathcal{N}$
Probability of event A	0.6110	0.6426	0.5774	0.6074	0.5132
Probability of event B	0.0265	0.0287	0.0261	0.0284	0.0251
Probability of event C	0.3625	0.3286	0.3965	0.3643	0.4617
Mean restricted time to B $E[T_{\mathbf{x}}^{B} 1_{\{T_{\mathbf{x}}^{B}<\infty\}}]$	0.2062	0.2355	0.1977	0.2264	0.1777
Mean restricted time to C $E[T_{\mathbf{x}}^{C} 1_{\{T_{\mathbf{x}}^{C}<\infty\}}]$	2.8283	2.8899	3.0782	3.1733	3.4914
Mean restricted time to $B \vee C$ $E[T_{\mathbf{x}}^{B\vee C} 1_{\{T_{\mathbf{x}}^{B\vee C}<\infty\}}]$	3.0345	3.1254	3.2759	3.3997	3.6692
Mean conditioned time to $B \vee C$ $E[T_{\mathbf{x}}^{B\vee C} \mid \{T_{\mathbf{x}}^{B\vee C} < \infty\}]$	7.8008	8.7452	7.7510	8.6586	7.5368

Finally, we can analyse the particular infectiousness of patient 1 in each scenario by analysing his exact reproduction number, $R_{\mathbf{x}}^{exact}(1)$. The probability mass function of this random variable, together with its mean, is plotted in Figure 6. When patient 1 is isolated, he will directly infect an average number of around 0.51 patients under any room configuration. The slight decrease of $E[R_{\mathbf{x}}^{exact}(1)]$ when room configuration changes from uncrowded to overcrowded settings represents that, under more crowded configurations, patient 1 plays a bit less important role in the spread of the epidemic. However, room configuration plays again a significant role when patient 1 is not isolated, so that $E[R_{\mathbf{x}}^{exact}(1)]$ varies between 1.1266 and 1.3718 depending on room con-

figuration. These results suggest that the isolation of patient 1 can reduce his infectiousness, measured in terms of $E[R_{\mathbf{x}}^{exact}(1)]$, up to more than a 50%.

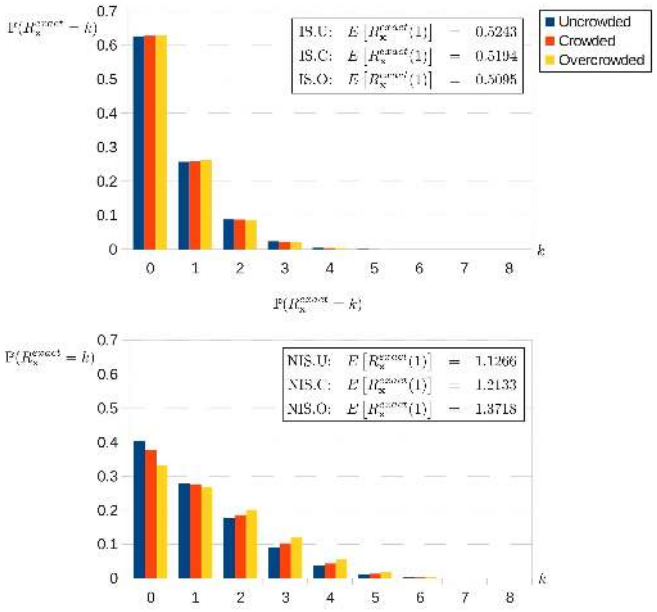

Fig. 6 Probability mass function of the exact reproduction number $R_{\mathbf{x}}^{exact}(1)$ for patient 1, and its mean, $E[R_{\mathbf{x}}^{exact}(1)]$, for isolation (*top*) and non-isolation (*bottom*) scenarios. Patient 1 initiates the outbreak, $\mathbf{x} = (I, S, \ldots, S)$

5 Discussion

In this paper, an SIR epidemic model for small heterogeneous populations has been analytically studied. In particular, the convenient definition of several stochastic descriptors, the application of first-step arguments, the construction of auxiliary absorbing Markov processes and the consideration of Laplace-Stieltjes transforms and probability generating functions, permit in Section 3 to study the dynamics of the spread of the epidemic among the individuals within the population in a similar manner than in [13] for the SIS epidemic model. However, in the SIR epidemic model both a scalar and a matrix-oriented approaches are feasible when analysing these descriptors. These approaches have been implemented here by means of two different labelling of states, Orders A and B, which permit to make use in different manners of the particular states transition structure of the process under study. In particular, by means of Order A which gives a pivotal role to individual N, we have developed an iterative scheme for the construction of the infinitesimal generator $\mathbf{Q}(N)$, which at the same time permits to obtain different matrices

involved in the solution of systems of equations for computing quantities of interest. Under this order, Algorithms 1M-3M following a matrix formalism can be obtained for the analysis of the stochastic descriptors in Section 3. On the other hand, we have followed for the scalar approach Order B, which is related to the lexicographic order for states within each sub-level. This order allows us to localise each state within its sub-level (Eq. (4)), yielding the scalar counterpart algorithms for computing the same quantities.

We illustrate in Section 4 our analysis by studying the spread of MRSA among the patients within an ICU. When a patient enters into the ICU carrying the infection, the spread of the disease within the ICU directly depends on several factors, such as the isolation of the patient and the room configuration of the ICU. We analyse this by considering six scenarios regarding those factors, and by analysing the stochastic descriptors described in Section 3. Main conclusions from Section 4 are:

- The isolation of the patient initiating the outbreak is the most effective measure for avoiding the spread of the epidemic, suggesting the importance of implementing appropriate screening policies for detecting infected individuals [40].
- Room configuration plays a more significant role when this isolation does not take place. This is a more general preventive measure that does not depend on the detection of the epidemic by screening policies. Room configuration then would be especially important in ICUs with limited resources (e.g., no isolation room) or when screening fails.
- Importance of isolation of patient 1 is also reflected when analysing the process from an individual perspective for the rest of the susceptible patients in the ICU, where sharing or not the room with patient 1 is pushed into the background.

Main simplifying assumption in Section 4 is that no discharge of patients is considered during the outbreak, which in our scenarios lasts for $\sim 11-16$ *days*. We may discuss here on the impact that this assumption has in our results. To this end, we consider now that susceptible and recovered individuals are discharged with rate $\mu = 0.1$ (average *length of stay* (*LOS*) equal to 10 *days*), and that they are immediately replaced by new patients, in the spirit of [4] and [11, Section 3]. From [4] we assume here that new admitted patients can carry MRSA with probability $\sigma = 0.01$, so that an especial variant of the classic SIRS epidemic model is constructed (new events in our process are $S \overset{\sigma\mu}{\to} I$, $R \overset{(1-\sigma)\mu}{\to} S$ and $R \overset{\sigma\mu}{\to} I$).

We focus here on the fate of a particular patient initially susceptible within the ICU, and carry out in Table 2 (by means of 10^4 stochastic simulations) the analogous analysis than in Table 1 when discharge and immediate admission of patients is considered. A direct comparison between results in Tables 1-2 show differences in the absolute values but yielding *qualitatively* similar relative behaviours and conclusions. Probability of a patient i not suffering the infection, $\mathbb{P}(A)$, increases in $0.1 - 0.25$ in any scenario in Table 2 with respect Table 1, which is directly related with the fact that patient i may be

discharged before becoming infected. Again, the network represents the most dangerous factor for the infection of any individual i, where the probability of a within-network infectious contact with patient i, $\mathbb{P}(C)$, slightly increases in more crowded situations. Similarly than in Table 1, isolation of patient 1 seems to be the most effective strategy for avoiding infection from an individual perspective: while $\mathbb{P}(A) = 0.7879$ for a patient sharing room with patient 1 in scenario NIS.U, this probability slightly increases up to 0.8130 for a patient not sharing room with patient 1, but it increases up to 0.8833 if patient 1 is isolated. On the other hand, mean restricted and conditioned times to infection of patient i ($E[T_{\mathbf{x}}^{B\vee C}1_{\{T_{\mathbf{x}}^{B\vee C}<\infty\}}]$ and $E[T_{\mathbf{x}}^{B\vee C}|T_{\mathbf{x}}^{B\vee C}<\infty]$) significantly decrease in Table 2 with respect the corresponding values in Table 1. This is directly related with the fact that the infection of patient i needs to occur *soon enough* before his potential discharge (which occurs, in average, after 10 *days*).

Table 2 Similar analysis than in Table 1, when discharge of patients is considered. Patient 1 initiates the outbreak, $\mathbf{x} = (I, S, \ldots, S)$. Fates of individual i: A: no infection; B: *external* infection; C: *within-network contact* infection; $B \vee C$: infection.

Isolated	IS.U	IS.C	IS.O
Fate of Patient i	$i \in \mathcal{N}$	$i \in \mathcal{N}$	$i \in \mathcal{N}$
Probability of event A	0.8833	0.8792	0.8667
Probability of event B	0.0182	0.0132	0.0159
Probability of event C	0.0985	0.1076	0.1174
Mean restricted time to B $E[T_{\mathbf{x}}^{B}1_{\{T_{\mathbf{x}}^{B}<\infty\}}]$	0.0764	0.0638	0.0661
Mean restricted time to C $E[T_{\mathbf{x}}^{C}1_{\{T_{\mathbf{x}}^{C}<\infty\}}]$	0.6302	0.6966	0.7440
Mean restricted time to $B \vee C$ $E[T_{\mathbf{x}}^{B\vee C}1_{\{T_{\mathbf{x}}^{B\vee C}<\infty\}}]$	0.7066	0.7604	0.8101
Mean conditioned time to $B \vee C$ $E[T_{\mathbf{x}}^{B\vee C}\|T_{\mathbf{x}}^{B\vee C}<\infty]$	6.0551	6.2949	6.0770

Non-isolated	NIS.U		NIS.C		NIS.O
Fate of Patient i	$i \in \{2,3\}$	$i \in \{4,\ldots,9\}$	$i \in \{2,\ldots,5\}$	$i \in \{6,\ldots,9\}$	$i \in \mathcal{N}$
Probability of event A	0.7879	0.8130	0.7564	0.7991	0.7301
Probability of event B	0.0138	0.0160	0.0128	0.0150	0.0130
Probability of event C	0.1983	0.1710	0.2308	0.1859	0.2569
Mean restricted time to B $E[T_{\mathbf{x}}^{B}1_{\{T_{\mathbf{x}}^{B}<\infty\}}]$	0.0582	0.0624	0.0565	0.0709	0.0524
Mean restricted time to C $E[T_{\mathbf{x}}^{C}1_{\{T_{\mathbf{x}}^{C}<\infty\}}]$	1.0091	0.9072	1.1451	1.0470	1.2759
Mean restricted time to $B \vee C$ $E[T_{\mathbf{x}}^{B\vee C}1_{\{T_{\mathbf{x}}^{B\vee C}<\infty\}}]$	1.0673	0.9696	1.2016	1.1179	1.3282
Mean conditioned time to $B \vee C$ $E[T_{\mathbf{x}}^{B\vee C}\|T_{\mathbf{x}}^{B\vee C}<\infty]$	5.0319	5.1849	4.9326	5.5646	4.9212

For analysing our process in this especial variant of the classic SIRS epidemic model, we have made use of 10^4 Gillespie simulations. We note that, when considering the potential adaptation of our arguments in this paper to the SIRS case considered in this section, the matrix approach seems to be the

only feasible one. The scalar approach followed for the SIR epidemic model needs to be seen as a *tailor-made* one, which is only possible thanks of the *forward-oriented* transition structure $S \to I \to R$ for events occurring to each individual in the population. Consideration of new *backward* events $R \overset{(1-\sigma)\mu}{\to} S$ and $R \overset{\sigma\mu}{\to} I$ would lead to new sub-blocks in the infinitesimal generator $\mathbf{Q}(N)$, and algorithms in Appendix C should be adapted.

We point out here that, as shown within this section, the use of stochastic simulations is an efficient way of approximating exact values computed in this paper, while our approach for computing these exact values entails high computational costs and is restricted to particular scenarios involving small population sizes. However, the analytical approach in this paper helps to understand the intrinsic differences between the SIR and other epidemic models, and to shed some light on the infinitesimal generators and the state spaces of the Markov chains corresponding to these models. In the particular case of the SIR epidemic model, a very particular quasi-birth-and-death process is obtained, and different population and individual descriptors can be proposed and analysed. The structure by levels and sub-levels allows one to analyse these descriptors by solving systems of linear equations, which has been done by means of a scalar and a matrix formulation and by using two labelling of the states, Order A and B. While alternative orders may be proposed, it is necessary that these orders allow the practical implementation of the systems of equations arising in Section 3, the construction of the infinitesimal generator if necessary, as well as the proper localisation of, at least, the initial state of interest within $\mathcal{S}$. The scalar and matrix approaches shown in this paper, implemented by means of Orders A and B, seem to be appropriate options fulfilling these conditions.

We have focused in Section 3 on analysing stochastic descriptors in the particular situation where $\gamma_i > 0$ for all $i \in \mathcal{N}$. However, other situations could be analysed with our approach while this is out of the scope of this paper. For example, the particular case in which a specific individual $i \in \mathcal{N}$ does not recover from the disease, so that $\gamma_i = 0$, can be analysed in a similar way by noting that some states $\mathbf{x} \in L^{(N)}(r;1)$, with $\mathbf{x}_i = I$, become absorbing. Then, descriptors could be analysed, for example, until the end of the outbreak or the arrival to these absorbing states. On the other hand, the definition of an outbreak, in Section 3, as the time until arriving to any state $\mathbf{y} \in L^{(N)}(r;0)$ for any $r \in \{1,\ldots,N\}$, which may not be absorbing, instead of for example considering the total time period until the process reaches an absorbing state, is clearly inspired in some applications such as the analysis of nosocomial infections in ICUs. In these kind of processes, it is usual that a particular outbreak, which lasts from some days to several weeks, will be followed by other ones during the following months and years in which probably different patients will be involved. Then, the interest is in analysing existing control measures during the particular time interval corresponding to an outbreak (that is, until the epidemic disappears from the ICU, regardless

of the potential future introduction of the epidemic again in the ICU by those remaining susceptible individuals, due to external sources).

Acknowledgements The author would like to thank the two anonymous referees for their careful consideration of this paper and their constructive comments. This work is supported by the Government of Spain (Ministry of Economy and Competitiveness) and the European Commission through the project MTM-2011-23864. The author is also supported by The Leverhulme Trust through the project with reference number RPG-2012-772. The author especially acknowledges Dr. Antonio Gómez-Corral (Complutense University of Madrid, Spain) for his helpful comments and suggestions to make the text more readable. Moreover, the author would like to acknowledge Dr. Antonis Economou (University of Athens, Greece) for the warm welcome he gave to him during his research visit to the University of Athens, when fruitful discussion took place and this research started. Author also acknowledges the University of Leeds for the permission to use the high performance computing facilities ARC1 and ARC2.

Appendix A. Notation

We introduce here some notation used throughout the paper. Regarding matrix notation, matrices and vectors are represented by bold letters, and given a matrix $\mathbf{A}$, $\mathbf{A}^T$ amounts to its transpose. $\mathbf{0}_{a\times b}$ represents a matrix of zeros with dimensions $a \times b$, while $\mathbf{e}_a$ represents a column vector of ones with dimension a. Moreover, $diag(a_1, \ldots, a_i)$ represents a diagonal matrix with elements $a_1, \ldots, a_i$ within its diagonal. Finally, given a set $\mathcal{S}$, $\#\mathcal{S}$ represents its cardinality, and $\delta_{i,j}$ is Kronecker's delta so that

$$\delta_{i,j} = \begin{cases} 0, & \text{if } i \neq j, \\ 1, & \text{if } i = j. \end{cases}$$

Appendix B. Iterative construction of $\mathbf{Q}(N)$ with Order A

The iterative procedure in this appendix is similar to the procedure for the construction of the infinitesimal generator in the SIS epidemic model [13]. In order to iteratively obtain the infinitesimal generator $\mathbf{Q}(N)$ corresponding to a population with N individuals, and following Order A for states within each sub-level, we first decompose $\mathbf{Q}(N)$ as a summation of three contributions regarding rates λ_i, γ_i and β_{ij}. In particular, each sub-matrix $\mathbf{Q}^{i,i'}_{r,r'}(N)$ for $(r', i') \in \{(r, i+1), (r+1, i-1)\}$ is split in

$$\mathbf{Q}^{i,i'}_{r,r'}(N) = \mathbf{Q}^{i,i';\lambda}_{r,r'}(N) + \mathbf{Q}^{i,i';\beta}_{r,r'}(N) + \mathbf{Q}^{i,i';\gamma}_{r,r'}(N),$$

so that $\mathbf{Q}^{i,i';\lambda}_{r,r'}(N)$ only contains the contribution of rates λ_k in matrix $\mathbf{Q}^{i,i'}_{r,r'}(N)$, and $\mathbf{Q}^{i,i';\beta}_{r,r'}(N)$ and $\mathbf{Q}^{i,i';\gamma}_{r,r'}(N)$ are related to the contribution of rates β_{ij} and γ_i, respectively. Then, they can be rewritten as $\mathbf{Q}^{i,i';\lambda}_{r,r'}(N, \underline{\boldsymbol{\lambda}}^{(N)})$, $\mathbf{Q}^{i,i';\beta}_{r,r'}(N, \mathbf{B}^{(N)})$ and $\mathbf{Q}^{i,i';\gamma}_{r,r'}(N, \underline{\boldsymbol{\gamma}}^{(N)})$

where

$$\underline{\boldsymbol{\lambda}}^{(N)} = \begin{pmatrix} \lambda_1 \\ \lambda_2 \\ \vdots \\ \lambda_{N-1} \\ \lambda_N \end{pmatrix} = \begin{pmatrix} \underline{\boldsymbol{\lambda}}^{(N-1)} \\ \lambda_N \end{pmatrix}, \quad \underline{\boldsymbol{\gamma}}^{(N)} = \begin{pmatrix} \gamma_1 \\ \gamma_2 \\ \vdots \\ \gamma_{N-1} \\ \gamma_N \end{pmatrix} = \begin{pmatrix} \underline{\boldsymbol{\gamma}}^{(N-1)} \\ \gamma_N \end{pmatrix}, \tag{B.1}$$

$$\mathbf{B}^{(N)} = \begin{pmatrix} 0 & \beta_{12} & \beta_{13} & \dots & \beta_{1N} \\ \beta_{21} & 0 & \beta_{23} & \dots & \beta_{2N} \\ \beta_{31} & \beta_{32} & 0 & \dots & \beta_{3N} \\ \vdots & \vdots & \vdots & \ddots & \vdots \\ \beta_{N1} & \beta_{N2} & \beta_{N3} & \dots & 0 \end{pmatrix} = \begin{pmatrix} \mathbf{B}^{(N-1)} & \underline{\boldsymbol{\beta}}_{\cdot N} \\ \underline{\boldsymbol{\beta}}_{N\cdot} & 0 \end{pmatrix},$$

with $\underline{\boldsymbol{\beta}}_{\cdot N} = \big(\beta_{1N}, \beta_{2N}, \dots, \beta_{N-1,N}\big)^T$, $\underline{\boldsymbol{\beta}}_{N\cdot} = \big(\beta_{N1}, \beta_{N2}, \dots, \beta_{N,N-1}\big)$.

The following iterative procedure permits the construction of matrices $\mathbf{Q}_{r,r'}^{i,i'}(N)$ by starting with matrices $\mathbf{Q}_{r,r'}^{i,i'}(M)$ corresponding to a population of $M = 1$ individual and increasing the value of M until the desired size $M = N$.

(a) For $M = 1$, $\underline{\boldsymbol{\lambda}}^{(M)} = (\lambda_1)$, $\underline{\boldsymbol{\gamma}}^{(M)} = (\gamma_1)$, and $\mathbf{B}^{(M)} = (0)$. Then,

$$\left.\begin{array}{l} \mathbf{Q}_{0,0}^{0,1,\lambda}(M, \underline{\boldsymbol{\lambda}}^{(M)}) = \underline{\boldsymbol{\lambda}}^{(M)}, \\ \mathbf{Q}_{0,0}^{0,1,\beta}(M, \mathbf{B}^{(M)}) = \mathbf{B}^{(M)}, \\ \mathbf{Q}_{0,0}^{0,1,\gamma}(M, \underline{\boldsymbol{\gamma}}^{(M)}) = (0), \end{array}\right\} \Rightarrow \begin{array}{l} \mathbf{Q}_{0,0}^{0,1}(M) = \mathbf{Q}_{0,0}^{0,1,\lambda}(M, \underline{\boldsymbol{\lambda}}^{(M)}) + \mathbf{Q}_{0,0}^{0,1,\beta}(M, \mathbf{B}^{(M)}) \\ + \mathbf{Q}_{0,0}^{0,1,\gamma}(M, \underline{\boldsymbol{\gamma}}^{(M)}) = (\lambda_1), \end{array}$$

$$\left.\begin{array}{l} \mathbf{Q}_{0,1}^{1,0,\lambda}(M, \underline{\boldsymbol{\lambda}}^{(M)}) = (0), \\ \mathbf{Q}_{0,1}^{1,0,\beta}(M, \mathbf{B}^{(M)}) = (0), \\ \mathbf{Q}_{0,1}^{1,0,\gamma}(M, \underline{\boldsymbol{\gamma}}^{(M)}) = \underline{\boldsymbol{\gamma}}^{(M)}, \end{array}\right\} \Rightarrow \begin{array}{l} \mathbf{Q}_{0,1}^{1,0}(M) = \mathbf{Q}_{0,1}^{1,0,\lambda}(M, \underline{\boldsymbol{\lambda}}^{(M)}) + \mathbf{Q}_{0,1}^{1,0,\beta}(M, \mathbf{B}^{(M)}) \\ + \mathbf{Q}_{0,1}^{1,0,\gamma}(M, \underline{\boldsymbol{\gamma}}^{(M)}) = (\gamma_1). \end{array}$$

(b) For $M = 2, \dots, N$, $\underline{\boldsymbol{\lambda}}^{(M)}$, $\underline{\boldsymbol{\gamma}}^{(M)}$ and $\mathbf{B}^{(M)}$ are obtained from the previously computed $\underline{\boldsymbol{\lambda}}^{(M-1)}$, $\underline{\boldsymbol{\gamma}}^{(M-1)}$ and $\mathbf{B}^{(M-1)}$ from $(B.1)$, and matrices $\mathbf{Q}_{r,r'}^{i,i'}(M)$ are computed as

$$\mathbf{Q}_{r,r'}^{i,i'}(M) = \mathbf{Q}_{r,r'}^{i,i',\lambda}(M, \underline{\boldsymbol{\lambda}}^{(M)}) + \mathbf{Q}_{r,r'}^{i,i',\beta}(M, \mathbf{B}^{(M)}) + \mathbf{Q}_{r,r'}^{i,i',\gamma}(M, \underline{\boldsymbol{\gamma}}^{(M)}),$$

where

– For $(r', i') = (r, i+1)$, $0 \le r \le M-1$ and $0 \le i \le M-r-1$, $\mathbf{Q}_{r,r}^{i,i+1,\gamma}(M, \underline{\boldsymbol{\gamma}}^{(M)}) = \mathbf{0}_{J^{(M)}(r;i)\times J^{(M)}(r;i+1)}$, while $\mathbf{Q}_{r,r}^{i,i+1,\lambda}(M, \underline{\boldsymbol{\lambda}}^{(M)})$ is given by

$$\begin{pmatrix} \mathbf{Q}_{r,r}^{i,i+1,\lambda}(M-1, \underline{\boldsymbol{\lambda}}^{(M-1)}) & \lambda_M \mathbf{I}_{J^{(M-1)}(r;i)} & \mathbf{0} \\ \mathbf{0} & \mathbf{Q}_{r,r}^{i-1,i,\lambda}(M-1, \underline{\boldsymbol{\lambda}}^{(M-1)}) & \mathbf{0} \\ \mathbf{0} & \mathbf{0} & \mathbf{Q}_{r-1,r-1}^{i,i+1,\lambda}(M-1, \underline{\boldsymbol{\lambda}}^{(M-1)}) \end{pmatrix} \tag{B.2}$$

and $\mathbf{Q}_{r,r}^{i,i+1,\beta}(M, \mathbf{B}^{(M)})$ has the form

$$\begin{pmatrix} \mathbf{Q}_{r,r}^{i,i+1,\beta}(M-1, \mathbf{B}^{(M-1)}) & \mathbf{U}_r^i(M-1) & \mathbf{0} \\ \mathbf{0} & \mathbf{Q}_{r,r}^{i-1,i,\beta}(M-1, \mathbf{B}^{(M-1)}) & \mathbf{0} \\ & + \mathbf{Q}_{r,r}^{i-1,i,\lambda}(M-1, \underline{\boldsymbol{\beta}}_{M\cdot}^T) & \\ \mathbf{0} & \mathbf{0} & \mathbf{Q}_{r-1,r-1}^{i,i+1,\beta}(M-1, \mathbf{B}^{(M-1)}) \end{pmatrix}. \tag{B.3}$$

We refer the reader to Remarks 1 and 2 for the details about matrices $\mathbf{Q}_{r,r}^{i-1,i,\lambda}(M-1, \underline{\boldsymbol{\beta}}_{M\cdot}^T)$ and $\mathbf{U}_r^i(M-1)$, respectively.

– For $(r',i')=(r+1,i-1)$, $0\leq r\leq M-1$ and $1\leq i\leq M-r$, $\mathbf{Q}_{r,r+1}^{i,i-1,\lambda}(M,\underline{\boldsymbol{\lambda}}^{(M)})=\mathbf{Q}_{r,r+1}^{i,i-1,\beta}(M,\mathbf{B}^{(M)})=\mathbf{0}_{J^{(M)}(r;i)\times J^{(M)}(r+1;i-1)}$, while $\mathbf{Q}_{r,r+1}^{i,i-1,\gamma}(M,\underline{\boldsymbol{\gamma}}^{(M)})$ is given by

$$\begin{pmatrix} \mathbf{Q}_{r,r+1}^{i,i-1,\gamma}(M-1,\underline{\boldsymbol{\gamma}}^{(M-1)}) & \mathbf{0} & \mathbf{0} \\ \mathbf{0} & \mathbf{Q}_{r,r+1}^{i-1,i-2,\gamma}(M-1,\underline{\boldsymbol{\gamma}}^{(M-1)}) & \gamma_M\mathbf{I}_{J^{(M-1)}(r;i-1)} \\ \mathbf{0} & \mathbf{0} & \mathbf{Q}_{r-1,r}^{i,i-1,\gamma}(M-1,\underline{\boldsymbol{\gamma}}^{(M-1)}) \end{pmatrix}. \quad (B.4)$$

Expressions $(B.2)$-$(B.4)$ are based on the nested level-structure of $\mathcal{S}$ in Order A. In particular, for a population of size N and any sub-level $L^{(N)}(r;i)$, it is verified that

$$L^{(N)}(r;i)=\left(L^{(N-1)}(r;i)\times\{S\}\right)\cup\left(L^{(N-1)}(r;i-1)\times\{I\}\right)\cup\left(L^{(N-1)}(r-1;i)\times\{R\}\right), \quad (B.5)$$

that is, possible states of a population with size N with i individuals infected and r individuals recovered can be explained in terms of the state of individuals $\{1,\ldots,N-1\}$ and individual N. Particular cases of expression $(B.5)$ appear for different combinations (r,i) regarding the values $r=0$, $r=N$, $i=0$ or $i=N-r$. Specifically,

– For $r=N$: $L^{(N)}(N;0)=L^{(N-1)}(N-1;0)\times\{R\}$.
– For $r=0$: $L^{(N)}(0;0)=L^{(N-1)}(0;0)\times\{S\}$, $L^{(N)}(0;N)=L^{(N-1)}(0;N-1)\times\{I\}$ and $L^{(N)}(0;i)=\left(L^{(N-1)}(0;i)\times\{S\}\right)\cup\left(L^{(N-1)}(0;i-1)\times\{I\}\right)$, for $1\leq i\leq N-1$,.
– For $1\leq r\leq N-1$: $L^{(N)}(r;0)=\left(L^{(N-1)}(r;0)\times\{S\}\right)\cup\left(L^{(N-1)}(r-1;0)\times\{R\}\right)$, $L^{(N)}(r;N-r)=\left(L^{(N-1)}(r;N-r-1)\times\{I\}\right)\cup\left(L^{(N-1)}(r-1;N-r)\times\{R\}\right)$,

so that expressions in our iterative procedure for computing matrices $\mathbf{Q}_{r,r'}^{i,i'}(M)$ have to be carefully implemented in these special cases, where some blocks of rows and/or columns should be removed.

Remark 1: Central sub-block $\mathbf{Q}_{r,r}^{i-1,i,\beta}(M-1,\mathbf{B}^{(M-1)})+\mathbf{Q}_{r,r}^{i-1,i,\lambda}(M-1,\underline{\boldsymbol{\beta}}_{M\cdot}^{T})$ in $(B.3)$ for the computation of matrix $\mathbf{Q}_{r,r}^{i,i+1,\beta}(M,\mathbf{B}^{(M)})$ stores infinitesimal transition rates corresponding to transitions from states in sub-level $L^{(M-1)}(r;i-1)\times\{I\}$ towards states in sub-level $L^{(M-1)}(r;i)\times\{I\}$. In particular, it only stores the contributions of rates in $\mathbf{B}^{(M)}$, that is, transitions representing an infection caused by an infectious contact within the network. Moreover, since we are considering here transitions from sub-level $L^{(M-1)}(r;i-1)\times\{I\}$ towards sub-level $L^{(M-1)}(r;i)\times\{I\}$, this infection is suffered by an individual in $\{1,\ldots,M-1\}$. This infection can be caused by another individual within $\{1,\ldots,M-1\}$, which yields the contribution $\mathbf{Q}_{r,r}^{i-1,i,\beta}(M-1,\mathbf{B}^{(M-1)})$, or it can be directly caused by individual M, so that it can be considered as an artificial external infection for the population $\{1,\ldots,M-1\}$, yielding contribution $\mathbf{Q}_{r,r}^{i-1,i,\lambda}(M-1,\underline{\boldsymbol{\beta}}_{M\cdot}^{T})$.

Remark 2: When computing the matrix $\mathbf{Q}_{r,r}^{i,i+1,\beta}(M,\mathbf{B}^{(M)})$, matrix $\mathbf{U}_r^i(M-1)$ stores infinitesimal transition rates corresponding to transitions from states of $L^{(M-1)}(r;i)\times\{S\}$ towards states of $L^{(M-1)}(r;i)\times\{I\}$, that is, transitions representing the infection of individual M due to an infectious contact with an individual within $\{1,\ldots,M-1\}$. We may construct this in terms of the auxiliary matrices $\mathbf{I}_r^i(M-1)$ from

$$\mathbf{U}_r^i(M-1)=diag\left(\mathbf{I}_r^i(M-1)\underline{\boldsymbol{\beta}}_{\cdot M}\right),$$

where matrices $\mathbf{I}_r^i(M-1)$ are recursively obtained as

$$\mathbf{I}_0^0(1)=\mathbf{I}_1^0(1)=(0),\quad \mathbf{I}_0^1(1)=(1),$$
$$\mathbf{I}_r^i(k)=\begin{pmatrix} \mathbf{I}_r^i(k-1) & \mathbf{0}_{J^{(k-1)}(r;i)} \\ \mathbf{I}_r^{i-1}(k-1) & \mathbf{e}_{J^{(k-1)}(r;i-1)} \\ \mathbf{I}_{r-1}^i(k-1) & \mathbf{0}_{J^{(k-1)}(r-1;i)} \end{pmatrix},\quad 0\leq r\leq k,\quad 0\leq i\leq k-r,$$

by properly removing the corresponding blocks of rows for boundary cases associated with $r=0$, $r=N$, $i=0$ or $i=N-r$.

Appendix C. Algorithms

Algorithm 1M (Restricted Laplace-Stieltjes transforms and moments of $T_{\mathbf{x}}(\bar{R})$, $\bar{R} \in \{1,\dots,N\}$. Order A)

For $\bar{R}=1,\dots,N$*:*
PART 1
$\mathbf{g}^1_{\bar{R}-1}(\bar{R};z)=\mathbf{A}^{1,0}_{\bar{R}-1,\bar{R}}(z)\mathbf{e}_{J(\bar{R};0)}$; $\mathbf{m}^{1,(0)}_{\bar{R}-1}(\bar{R})=\mathbf{g}^1_{\bar{R}-1}(\bar{R};0)$;
For $r=\bar{R}-2,\dots,0$*:*
$\mathbf{g}^{\bar{R}-r}_r(\bar{R};z)=\mathbf{A}^{\bar{R}-r,\bar{R}-r-1}_{r,r+1}(z)\mathbf{g}^{\bar{R}-r-1}_{r+1}(\bar{R};z)$; $\mathbf{m}^{\bar{R}-r,(0)}_r(\bar{R})=\mathbf{g}^{\bar{R}-r}_r(\bar{R};0)$;
For $i=\bar{R}-r-1,\dots,2$*:*
$\mathbf{g}^i_r(\bar{R};z)=\mathbf{A}^{i,i+1}_{r,r}(z)\mathbf{g}^{i+1}_r(\bar{R};z)+\mathbf{A}^{i,i-1}_{r,r+1}(z)\mathbf{g}^{i-1}_{r+1}(\bar{R};z)$; $\mathbf{m}^{i,(0)}_r(\bar{R})=\mathbf{g}^i_r(\bar{R};0)$;
$\mathbf{g}^1_r(\bar{R};z)=\mathbf{A}^{1,2}_{r,r}(z)\mathbf{g}^2_r(\bar{R};z)$; $\mathbf{m}^{1,(0)}_r(\bar{R})=\mathbf{g}^1_r(\bar{R};0)$;
PART 2
For $p=1,\dots,l$*:*
$\mathbf{m}^{1,(p)}_{\bar{R}-1}(\bar{R})=p\tilde{\mathbf{m}}^{1,(p-1)}_{\bar{R}-1}(\bar{R})$;
For $r=\bar{R}-2,\dots,0$*:*
$\mathbf{m}^{\bar{R}-r,(p)}_r(\bar{R})=\mathbf{A}^{\bar{R}-r,\bar{R}-r-1}_{r,r+1}(0)\mathbf{m}^{\bar{R}-r-1,(p)}_{r+1}(\bar{R})+p\tilde{\mathbf{m}}^{\bar{R}-r,(p-1)}_r(\bar{R})$;
For $i=\bar{R}-r-1,\dots,2$*:*
$\mathbf{m}^{i,(p)}_r(\bar{R})=\mathbf{A}^{i,i+1}_{r,r}(0)\mathbf{m}^{i+1,(p)}_r(\bar{R})+\mathbf{A}^{i,i-1}_{r,r+1}(0)\mathbf{m}^{i-1,(p)}_{r+1}(\bar{R})+p\tilde{\mathbf{m}}^{i,(p-1)}_r(\bar{R})$;
$\mathbf{m}^{1,(p)}_r(\bar{R})=\mathbf{A}^{1,2}_{r,r}(0)\mathbf{m}^{2,(p)}_r(\bar{R})+p\tilde{\mathbf{m}}^{1,(p-1)}_r(\bar{R})$;

Vectors $\tilde{\mathbf{m}}^{i,(p)}_r(\bar{R})$ in Algorithm 1M (Part 2) are obtained by dividing each $\mathbf{x}$th row of $\mathbf{m}^{i,(p)}_r(\bar{R})$ by $q_{\mathbf{x}}$.

Algorithm 1S (Laplace-Stieltjes transforms and moments of $T_{\mathbf{x}}(\bar{R})$, $\bar{R}\in\{1,\dots,N\}$. Order B)

For $\bar{R}=1,\dots,N$*:*
PART 1
For $r=\bar{R}-1,\dots,0$*:*
For $i=\bar{R}-r,\dots,1$*:*
For any $\mathbf{x}=\{(a_1,\dots,a_i),(b_1,\dots,b_r)\}$*:*
Compute $\phi^{(a_1,\dots,a_i)}_{(b_1,\dots,b_r)}(\bar{R};z)$ *from Eq.* (10) *and store it in position* $Pos^i_r(\mathbf{x})$ *(from* (4)*) of vector* $\mathbf{g}^i_r(\bar{R};z)$;
$\mathbf{m}^{i,(0)}_r(\bar{R})=\mathbf{g}^i_r(\bar{R};0)$;
PART 2
For $p=1,\dots,l$*:*
For $r=\bar{R}-1,\dots,0$*:*
For $i=\bar{R}-r,\dots,1$*:*
For any $\mathbf{x}=\{(a_1,\dots,a_i),(b_1,\dots,b_r)\}$*:*
Compute $m^{(a_1,\dots,a_i),(p)}_{(b_1,\dots,b_r)}(\bar{R})$ *from Eq.* (11) *and store it in position* $Pos^i_r(\mathbf{x})$ *(from* (4)*) of vector* $\mathbf{m}^{i,(p)}_r(\bar{R})$;

Algorithm 2M (Laplace-Stieltjes transforms and moments of $T^I_{\mathbf{x}}$, $I\geq \#I(\mathbf{x})$. Order A)

For $I=2,\dots,N$*:*
PART 1
$\mathbf{h}^{I-1}_{N-I}(I;z)=\mathbf{A}^{I-1,I}_{N-I,N-I}(z)\mathbf{e}_{J(N-I;I)}$; $\mathbf{n}^{I-1,(0)}_{N-I}(I)=\mathbf{h}^{I-1}_{N-I}(I;0)$;
For $i=I-2,\dots,1$*:*
$\mathbf{h}^i_{N-I}(I;z)=\mathbf{A}^{i,i+1}_{N-I,N-I}(z)\mathbf{h}^{i+1}_{N-I}(I;z)$; $\mathbf{n}^{i,(0)}_{N-I}(I)=\mathbf{h}^i_{N-I}(I;0)$;
For $r=N-I-1,\dots,0$*:*
$\mathbf{h}^{I-1}_r(I;z)=\mathbf{A}^{I-1,I-2}_{r,r+1}(z)\mathbf{h}^{I-2}_{r+1}(I;z)+\mathbf{A}^{I-1,I}_{r,r}(z)\mathbf{e}_{J(r;I)}$; $\mathbf{n}^{I-1,(0)}_r(I)=\mathbf{h}^{I-1}_r(I;0)$;
For $i=I-2,\dots,2$*:*
$\mathbf{h}^i_r(I;z)=\mathbf{A}^{i,i-1}_{r,r+1}(z)\mathbf{h}^{i-1}_{r+1}(I;z)+\mathbf{A}^{i,i+1}_{r,r}(z)\mathbf{h}^{i+1}_r(I;z)$; $\mathbf{n}^{i,(0)}_r(I)=\mathbf{h}^i_r(I;0)$;
$\mathbf{h}^1_r(I;z)=\mathbf{A}^{1,2}_{r,r}(z)\mathbf{h}^2_r(I;z)$; $\mathbf{n}^{1,(0)}_r(I)=\mathbf{h}^1_r(I;0)$;

PART 2
For $p = 1, \ldots, l$*:*
$\mathbf{n}_{N-I}^{I-1,(p)}(I) = p\tilde{\mathbf{n}}_{N-I}^{I-1,(p-1)}(I)$*;*
For $i = I-2, \ldots, 1$*:*
$\mathbf{n}_{N-I}^{i,(p)}(I) = \mathbf{A}_{N-I,N-I}^{i,i+1}(0)\mathbf{n}_{N-I}^{i+1,(p)}(I) + p\tilde{\mathbf{n}}_{N-I}^{i,(p-1)}(I)$*;*
For $r = N-I-1, \ldots, 0$*:*
$\mathbf{n}_{r}^{I-1,(p)}(I) = \mathbf{A}_{r,r+1}^{I-1,I-2}(0)\mathbf{n}_{r+1}^{I-2,(p)}(I) + p\tilde{\mathbf{n}}_{r}^{I-1,(p-1)}(I)$*;*
For $i = I-2, \ldots, 2$*:*
$\mathbf{n}_{r}^{i,(p)}(I) = \mathbf{A}_{r,r+1}^{i,i-1}(0)\mathbf{n}_{r+1}^{i-1,(p)}(I) + \mathbf{A}_{r,r}^{i,i+1}(0)\mathbf{n}_{r}^{i+1,(p)}(I) + p\tilde{\mathbf{n}}_{r}^{i,(p-1)}(I)$*;*
$\mathbf{n}_{r}^{1,(p)}(I) = \mathbf{A}_{r,r}^{1,2}(0)\mathbf{n}_{r}^{2,(p)}(I) + p\tilde{\mathbf{n}}_{r}^{1,(p-1)}(I)$*;*

Vectors $\tilde{\mathbf{n}}_{r}^{i,(p)}(I)$ in Algorithm 2M (Part 2) are obtained by dividing each $\mathbf{x}$th row of $\mathbf{n}_{r}^{i,(p)}(I)$ by $q_{\mathbf{x}}$.

Algorithm 2S (Laplace-Stieltjes transforms and moments of $T_{\mathbf{x}}^{I}$, $I \geq \#I(\mathbf{x})$. Order B)

For $I = 2, \ldots, N$*:*
PART 1
For $r = N-I, \ldots, 0$*:*
For $i = I-1, \ldots, 1$*:*
For any $\mathbf{x} = \{(a_1, \ldots, a_i), (b_1, \ldots, b_r)\}$*:*
Compute $\varphi_{(b_1,\ldots,b_r)}^{(a_1,\ldots,a_i)}(I; z)$ *from scalar version of Eq.* (12) *and store it in position* $Pos_r^i(\mathbf{x})$ *(from* (4)*) of vector* $\mathbf{h}_r^i(I; z)$*;*
$\mathbf{n}_{r}^{i,(0)}(I) = \mathbf{h}_{r}^{i}(I; 0)$*;*
PART 2
For $p = 1, \ldots, l$*:*
For $r = N-I, \ldots, 0$*:*
For $i = I-1, \ldots, 1$*:*
For any $\mathbf{x} = \{(a_1, \ldots, a_i), (b_1, \ldots, b_r)\}$*:*
Compute $n_{(b_1,\ldots,b_r)}^{(a_1,\ldots,a_i),(p)}(I)$ *by differentiating scalar version of Eq.* (12) *and store it in position* $Pos_r^i(\mathbf{x})$ *(from* (4)*) of vector* $\mathbf{n}_{r}^{i,(p)}(I)$*;*

Algorithm 3M (Probability generating functions and factorial moments of $R_{\mathbf{x}}^{exact}$. Order A)

PART 1
$\boldsymbol{\mu}_{N-2}^{2}(s) = \mathbf{e}_{J^{(N-1)}(N-2;1)}$**;** $\bar{\mathbf{v}}_{N-2}^{2,(0)} = \boldsymbol{\mu}_{N-2}^{2}(1)$**;**
$\boldsymbol{\mu}_{N-2}^{1}(s) = \left(\bar{\mathbf{A}}_{N-2,N-2}^{1,2} + s\mathbf{Q}_{N-2,N-2}^{0,1,\lambda}(N-1, \underline{\beta}_{N\cdot}^{T})\right)\boldsymbol{\mu}_{N-2}^{2}(s) + \bar{\mathbf{c}}_{N-2}^{1}$**;** $\bar{\mathbf{v}}_{N-2}^{1,(0)} = \boldsymbol{\mu}_{N-2}^{1}(1)$**;**
For $r = N-3, \ldots, 0$*:*
$\boldsymbol{\mu}_{N-r}^{r}(s) = \mathbf{e}_{J^{(N-1)}(r;N-r-1)}$*;* $\bar{\mathbf{v}}_{N-r}^{r,(0)} = \boldsymbol{\mu}_{N-r}^{r}(1)$*;*
For $i = N-r-1, \ldots, 2$*:*
$\boldsymbol{\mu}_{r}^{i}(s) = \left(\bar{\mathbf{A}}_{r,r}^{i,i+1} + s\mathbf{Q}_{r,r}^{i-1,i,\lambda}(N-1, \underline{\beta}_{N\cdot}^{T})\right)\boldsymbol{\mu}_{r}^{i+1}(s) + \bar{\mathbf{A}}_{r,r+1}^{i,i-1}\boldsymbol{\mu}_{r+1}^{i-1}(s) + \bar{\mathbf{c}}_{r}^{i}$*;*
$\bar{\mathbf{v}}_{r}^{i,(0)} = \boldsymbol{\mu}_{r}^{i}(1)$*;*
$\boldsymbol{\mu}_{r}^{1}(s) = \left(\bar{\mathbf{A}}_{r,r}^{1,2} + s\mathbf{Q}_{r,r}^{0,1,\lambda}(N-1, \underline{\beta}_{N\cdot}^{T})\right)\boldsymbol{\mu}_{r}^{2}(s) + \bar{\mathbf{c}}_{r}^{1}$*;* $\bar{\mathbf{v}}_{r}^{1,(0)} = \boldsymbol{\mu}_{r}^{1}(1)$*;*
PART 2
For $p = 1, \ldots, l$*:*
$\bar{\mathbf{v}}_{N-2}^{1,(p)} = p\mathbf{Q}_{N-2,N-2}^{0,1,\lambda}(N-1, \underline{\beta}_{N\cdot}^{T})\bar{\mathbf{v}}_{N-2}^{2,(p-1)}$*;*
For $r = N-3, \ldots, 0$*:*
$\bar{\mathbf{v}}_{N-r}^{r,(p)} = \mathbf{0}_{J^{(N-1)}(r;N-r-1)}$*;*
For $i = N-r-1, \ldots, 2$*:*
$\bar{\mathbf{v}}_{r}^{i,(p)} = \left(\bar{\mathbf{A}}_{r,r}^{i,i+1} + \mathbf{Q}_{r,r}^{i-1,i,\lambda}(N-1, \underline{\beta}_{N\cdot}^{T})\right)\bar{\mathbf{v}}_{r}^{i+1,(p)} + \bar{\mathbf{A}}_{r,r+1}^{i,i-1}\bar{\mathbf{v}}_{r+1}^{i-1,(p)} + \mathbf{Q}_{r,r}^{i-1,i,\lambda}(N-1, \underline{\beta}_{N\cdot}^{T})p\bar{\mathbf{v}}_{r}^{i+1,(p-1)}$*;*
$\bar{\mathbf{v}}_{r}^{1,(p)} = \left(\bar{\mathbf{A}}_{r,r}^{1,2} + \mathbf{Q}_{r,r}^{0,1,\lambda}(N-1, \underline{\beta}_{N\cdot}^{T})\right)\bar{\mathbf{v}}_{r}^{2,(p)} + \mathbf{Q}_{r,r}^{0,1,\lambda}(N-1, \underline{\beta}_{N\cdot}^{T})p\bar{\mathbf{v}}_{r}^{2,(p-1)}$*;*

Algorithms in this appendix allow one to compute the measures analysed in Section 3, regarding population and individual stochastic descriptors for the epidemic process within the network. These algorithms have been developed here with the scalar (Algorithms 1S and 2S) and matrix (Algorithms 1M, 2M and 3M) approach, and their implementation in Python is available in [27].

We present in Table C.1 a detailed description of the computations carried out within each algorithm in this appendix, in order to discuss on the convenience of implementing the scalar or the matrix-oriented algorithms, and to understand the complexity of analysing each stochastic descriptor in this paper. At first glance, Table C.1 allows one to notice that population descriptors analysed in Algorithms 1S-1M and 2S-2M amount, in general, to higher computational efforts than, for example, analysing the individual descriptor $R_{\mathbf{x}}^{exact}$ in Algorithm 3M. This is due to the fact that random variables $T_{\mathbf{x}}(\bar{R})$ and $T_{\mathbf{x}}^{I}$ need to be studied for the different values of $\bar{R}$ and I. When comparing between the computational demand of scalar-oriented algorithms versus their matrix counterparts, description in Table C.1 suggests that these are qualitatively similar. For example, while each iteration in Algorithm 1S amounts to the implementation of the scalar Eq. (10) (or (11)), and needs to be done $\binom{N}{r|i}$ times corresponding to the possible states in $L^{(N)}(r;i)$, this is substituted in Algorithm 1M by a single iteration amounting to the implementation of the matrix equation corresponding to Eq. (7) (or its derivatives) for sub-level $L^{(N)}(r;i)$, which involves the product of matrices and vectors with dimensions $\binom{N}{r|i}$.

It is worth to point out that, however, and especially for higher values of N, a poorer computational performance of Algorithms 1M and 2M versus their scalar counterparts 1S and 2S, respectively, is expected. This is because the following main reasons: (i) matrix-oriented algorithms in this section require the prior construction of infinitesimal generator $\mathbf{Q}(N)$ (Appendix B) and related matrices; (ii) implementation of, for example, the matrix equation arising from Eq. (7) involves the multiplication of large sparse matrices an vectors where many unnecessary computations are carried out (this could be improved by means of specialised methods for dealing with this kind of matrices [45]); and (iii) in terms of memory requirements, the storage of infinitesimal generator $\mathbf{Q}(N)$ (square matrix with dimensions $3^N \times 3^N$) and related matrices is clearly inefficient in comparison with scalar approaches.

In Table C.2, we present a computational comparison between Algorithms 2S and 2M when implemented for an homogeneous population of size N, which has been carried out with Python programming language and in a high performance computing facility -quad-core AMD 8384 (2.7 Ghz) processor with $32GB$ of $DDR2$ memory- of the University of Leeds. It can be observed that Algorithm 2M computes the desired quantity in less time and using less memory than Algorithm 2S for small values of N. However, for increasing values of N the performance of Algorithm 2S improves, permitting to compute the desired quantities for larger values of N, in less time and demanding considerably less memory than Algorithm 2M. For the sake of completeness, we incorporate in Table C.2 a third alternative: to solve matrix equations arising from Section 3 by standard procedures, which would be the way to proceed if the structure of the coefficient matrix were not to be exploited. In particular, computational performance of this alternative is presented in Table C.2 when the standard *numpy.linalg.solve* solver from Python is used (which, at the same time, makes use of the *gesv* LAPACK routine). Computational performance differences in Table C.2 are only quantitative, where the scalar approach seems to be the best option. However, we point out that this scalar approach is a *tailor-made* one directly based in the *forward-oriented* transition structure of the SIR epidemic model, $S \to I \to R$, which seems not to be generalisable to other more complex epidemic models, where matrix-oriented approaches should prevail [13, 39]. We point out here that additional efforts may be made when implementing algorithms in this appendix [27], which is out of the scope of this paper. However, at the light of the results in Table C.2, and regardless of the labelling of states and the particular approach followed, our method should be considered as purely theoretical for values of N far beyond 15, which amount to CTMCs with more than 4×10^7 states.

Table C.1 Computational complexity summary of Algorithms 1S, 1M, 2S, 2M, 3M and the construction of $\mathbf{Q}(N)$ from Appendix B.

Algorithm 1S	**Algorithm 1M**
• Computes Laplace-Stieltjes transform and moments of $T_{\mathbf{x}}(\bar{R})$, from Eqs. (10)-(11). • It consists of 5 nested loops, yielding a total number of $(l+1)\sum_{\bar{R}=1}^{N}\sum_{r=0}^{\bar{R}-1}\sum_{i=1}^{\bar{R}-r}\binom{N}{r\|i}$ iterations. • Each iteration involves implementing a scalar equation (Eq. (10) or (11)).	• Computes Laplace-Stieltjes transform and moments of $T_{\mathbf{x}}(\bar{R})$, from Eq. (7) and its derivatives. • It consists of 4 nested loops, yielding a total number of $(l+1)\sum_{\bar{R}=1}^{N}\sum_{r=0}^{\bar{R}-1}\sum_{i=1}^{\bar{R}-r}1$ iterations. • Each iteration involves implementing a matrix equation (Eq. (7) or its derivatives), for sub-level $L^{(N)}(r;i)$, involving multiplication of matrices and vectors of dimension $\binom{N}{r\|i}$.
Algorithm 2S	**Algorithm 2M**
• Computes Laplace-Stieltjes transform and moments of $T^I_{\mathbf{x}}$, from the scalar version of Eq. (12), and its derivatives. • It consists of 5 nested loops, yielding a total number of $(l+1)\sum_{I=1}^{N}\sum_{r=0}^{N-I}\sum_{i=1}^{I-1}\binom{N}{r\|i}$ iterations. • Each iteration involves implementing a scalar equation (scalar version of Eq. (12), or its derivatives for moments).	• Computes Laplace-Stieltjes transform and moments of $T^I_{\mathbf{x}}$, from Eq. (12) and its derivatives. • It consists of 4 nested loops, yielding a total number of $(l+1)\sum_{I=1}^{N}\sum_{r=0}^{N-I}\sum_{i=1}^{I-1}1$ iterations. • Each iteration involves implementing a matrix equation (Eq. (12) or its derivatives), for sub-level $L^{(N)}(r;i)$, involving multiplication of matrices and vectors of dimension $\binom{N}{r\|i}$.
Construction of $\mathbf{Q}(N)$	**Algorithm 3M**
• Computes the infinitesimal generator $\mathbf{Q}(N)$ from procedure in Appendix B. • It consists of a loop for $M=1,\ldots,N$, where at each iteration we do: • Create $\underline{\boldsymbol{\lambda}}^{(M)}$, $\underline{\boldsymbol{\gamma}}^{(M)}$ and $\mathbf{B}^{(M)}$ from (B.1), with dimensions $M\times 1$, $M\times 1$ and $M\times M$. • Create matrices $\mathbf{Q}^{i,i+1,\lambda}_{r,r}(M,\underline{\boldsymbol{\lambda}}^{(M)})$, $\mathbf{Q}^{i,i+1,\beta}_{r,r}(M,\mathbf{B}^{(M)})$, and $\mathbf{Q}^{i,i-1,\gamma}_{r,r+1}(M,\underline{\boldsymbol{\gamma}}^{(M)})$ from $(B.2)-(B.4)$. This involves filling matrices with dimensions $\binom{M}{r\|i}\times\binom{M}{r\|i+1}$, $\times\binom{M}{r\|i+1}$, and $\times\binom{M}{r+1\|i-1}$, respectively. • Create matrices $I^i_r(M)$, $0\le r\le M$, $0\le i\le M-r$, recursively from Appendix B. This involves filling matrices (by-blocks) with dimensions $\binom{M}{r\|i}\times M$. From each $I^i_r(M)$, we create matrix $U^i_r(M)$ from Appendix B, with dimensions $\binom{M}{r\|i}\times\binom{M}{r\|i}$.	• Computes the probability generating function and factorial moments of $R^{exact}_{\mathbf{x}}$, from Eq. (15) and its derivatives. • It consists of 3 nested loops, yielding a total number of $(l+1)\sum_{r=0}^{N-2}\sum_{i=1}^{N-r}1$ iterations. • Each iteration involves implementing a matrix equation (Eq. (15) or its derivatives), for sub-level $L^{(N)}(r;i)$, involving multiplication of matrices and vectors of dimension $\binom{N-1}{r\|i-1}$.

Table C.2 Computational comparison (time, in *seconds*, and memory usage, in *megabytes*) between Algorithm 2S, 2M and the solution given by a standard solver. Homogeneous population with N individuals. $\lambda_i = 1$, $\gamma_i = 3$ for all $i \in \mathcal{N}$, $\beta_{ij} = 2$ for all $(i,j) \in \mathcal{L}$

	N	4	5	6	7	8
$E\left[I^{max}_{(I,S,S,\ldots,S)}\right]$		2.5090	3.1029	3.7490	4.4414	5.1729
Time	*Alg. 2S*	0.08	0.44	2.41	11.64	52.49
	Alg. 2M	0.01	0.1	0.71	5.66	49.06
	Standard Solver	0.01	0.12	1.06	9.72	109.48
Memory	*Alg. 2S*	< 15	18.29	18.36	18.59	19.20
Usage	*Alg. 2M*	< 15	< 15	19.01	28.48	107.04
	Standard Solver	< 15	< 15	19.01	39.03	442.35
	N	9	10	11	12	13
$E\left[I^{max}_{(I,S,S,\ldots,S)}\right]$		5.9368	6.7272	7.5393	8.3695	9.2146
Time	*Alg. 2S*	201.78	834.78	3647.25	13102.28	49655.32
	Alg. 2M	330.39	2783.13	–	–	–
	Standard Solver	1088.14	–	–	–	–
Memory	*Alg. 2S*	21.02	25.33	38.23	77.23	200.29
Usage	*Alg. 2M*	701.48	5653.00	$> 32GB$	$> 32GB$	$> 32GB$
	Standard Solver	5493.76	$> 32GB$	$> 32GB$	$> 32GB$	$> 32GB$

Conflict of Interest: The author declares that he has no conflict of interest.

References

1. Abate J, Whitt W (1992) Numerical inversion of probability generating functions. Operations Research Letters 12: 245-251.
2. Allen LJS (2003) An introduction to stochastic processes with applications to biology. Pearson Education, New Jersey.
3. Artalejo JR, Lopez-Herrero MJ (2013) On the exact measure of the disease spread in stochastic epidemic models. Bulletin of Mathematical Biology 75: 1031-1050.
4. Artalejo JR (2014) On the Markovian approach for modeling the dynamics of nosocomial Infections. Acta Biotheoretica 62: 15-34.
5. Austin DJ, Anderson RM (1999) Studies of antibiotic resistance within the patient, hospitals and the community using simple mathematical models. Philosophical Transactions of the Royal Society of London. Series B: Biological Sciences 354: 721-738.
6. Ball FG (1999) Stochastic and deterministic models for SIS epidemics among a population partitioned into households. Mathematical Biosciences 156: 41-67.
7. Ball FG, Britton T, Lyne OD (2004) Stochastic multitype epidemics in a community of households: estimation of threshold parameter R and secure vaccination coverage. Biometrika 91: 345-362.
8. Ball FG, Britton T (2007) An epidemic model with infector-dependent severity. Advances in Applied Probability 39: 949-972.
9. Brimblecombe FSW, Cruickshank R, Masters PL, Reid DD (1958) Family studies of respiratory infections. British Medical Journal 18: 119-128.
10. Britton T (2010) Stochastic epidemic models: a survey. Mathematical Biosciences 225: 24-35.
11. Cooper BS, Lipsitch M (2004) The analysis of hospital infection data using hidden Markov models. Biostatistics 5: 223-237.
12. Deijfen M (2011) Epidemics and vaccination on weighted graphs. Mathematical Biosciences 232: 57-65.

13. Economou A, Gómez-Corral A, López-García M (2015) A stochastic SIS epidemic model with heterogeneous contacts. Physica A 421: 78-97.
14. Forrester M, Pettitt AN (2005) Use of stochastic epidemic modeling to quantify transmission rates of colonization with Methicillinresistant Staphylococcus aureus in an intensive care unit. Infection Control and Hospital Epidemiology 26: 598-606.
15. Funk S, Salathé M, Jansen VAA (2010) Modelling the influence of human behaviour on the spread of infectious diseases: a review. Journal of The Royal Society Interface 7: 1247-1256.
16. Gillespie, DT (1977) Exact stochastic simulation of coupled chemical reactions. The Journal of Physical Chemistry 81: 2340-2361.
17. Grimwood K, Abbott GD, Fergusson DM, Jennings LC, Allan JM (1983) Spread of rotavirus within families: a community based study. British Medical Journal 287: 575-577.
18. Hatzopoulos V, Taylor M, Simon PL, Kiss IZ (2011) Multiple sources and routes of information transmission: implications for epidemic dynamics. Mathematical Biosciences 231: 197-209.
19. Hill AN, Longini Jr IM (2003) The critical vaccination fraction for heterogeneous epidemic models. Mathematical Biosciences 181: 85-106.
20. Hotta LK (2010) Bayesian melding estimation of a stochastic SEIR model. Mathematical Population Studies 17: 101-111.
21. Jenkinson G, Goutsias J (2012) Numerical integration of the master equation in some models of stochastic epidemiology. PLoS ONE 7: e36160.
22. Kermack WO, McKendrick AG (1927) A contribution to the mathematical theory of epidemics. In: Proceedings of the Royal Society of London A: Mathematical, Physical and Engineering Sciences 115: 700-721.
23. Kiss IZ, Cassell J, Recker M, Simon PL (2010) The impact of information transmission on epidemic outbreaks. Mathematical Biosciences 225: 1-10.
24. Latouche G, Ramaswami V (1999) Introduction to matric analytic methods in stochastic modeling. ASA-SIAM, Philadelphia.
25. Li C, van de Bovenkamp R, Van Mieghem P (2012) Susceptible-infected-susceptible model: a comparison of N-intertwined and heterogeneous mean-field approximations. Physical Review E 86: 026116 (9 pages).
26. Liu C, Bayer A, Cosgrove SE, Daum RS, Fridkin SK, Gorwitz RJ, Kaplan SL, Karchmer AW, Levine DP, Murray BE, Rybak MJ, Talan DA, Chambers HF (2011) Clinical practice guidelines by the infectious diseases society of america for the treatment of Methicillin-resistant staphylococcus aureus infections in adults and children. Clinical Infectious Diseases: ciq146
27. López-García M (2015) Supplementary material on "Stochastic Descriptors in an SIR Epidemic Model for Heterogeneous Individuals in Small Networks". http://dx.doi.org/***. [Python .py files will be available from the web page of the journal. Nowadays, they can be found in https://www1.maths.leeds.ac.uk/~lopezgarcia/Algorithms.html]
28. McBryde ES, Pettitt AN, McElwain DLS (2007) A stochastic mathematical model of methicillin resistant Staphylococcus aureus transmission in an intensive care unit: predicting the impact of interventions. Journal of Theoretical Biology 245: 470-481.
29. Moler C, Van Loan C (2003) Nineteen dubious ways to compute the exponential of a matrix, twenty-five years later. SIAM Review 20: 801-836.
30. Newmann MEJ (2010) Networks. An introduction. Oxford University Press, Oxford.
31. Pastor-Satorras R, Vespignani A (2001) Epidemic dynamics and endemic states in complex networks. Physical Review Letters E 63: 066117 (8 pages).
32. Pastor-Satorras R, Vespignani A (2002) Epidemic dynamics in finite size scale-free networks. Physical Review Letters E 65: 035108 (4 pages).
33. Roberts M, Andreasen V, Lloyd L, Pellis L (2014) Nine challenges for deterministic epidemic models. Epidemics. doi:10.1016/j.epidem.2014.09.006
34. Ross JV (2011) Invasion of infectious diseases in finite homogeneous populations. Journal of Theoretical Biology 289: 83-89.
35. Sahneh FD, Scoglio C, Van Mieghem P (2013) Generalized epidemic mean-field model for spreading processes over multilayer complex networks. IEEE/ACM Transactions on Networking, 21: 1609-1620.

36. Saunders IW (1981) Epidemics in competition. Journal of Mathematical Biology 11: 311-318.
37. Shapiro M, Delgado-Eckert E (2012) Finding the probability of infection in an SIR network is NP-Hard. Mathematical Biosciences 240: 77-84.
38. Sidje RB (1998) EXPOKIT: A software package for computing matrix exponentials. ACM Transactions on Mathematical Software 24: 130-156.
39. Simon PL, Taylor M, Kiss IZ (2011) Exact epidemic models on graphs using graph-automorphism driven lumping. Journal of Mathematical Biology 62: 479-508.
40. Trapman P, Bootsma MCJ (2009) A useful relationship between epidemiology and queueing theory: the distribution of the number of infectives at the moment of the first detection. Mathematical Biosciences 219: 15-22.
41. Valentin A, Ferdinande P (2011) Recommendations on basic requirements for intensive care units: structural and organizational aspects. Intensive Care Medicine 37: 1575-1587.
42. Van Mieghem P, Omic J, Kooij R (2009) Virus spread in networks. IEEE/ACM Transactions on Networking 17: 1-14.
43. Watts DJ, Strogatz SH (1998) Collective dynamics of 'small-world' networks. Nature 393: 440-442.
44. White H, Martín del Rey A, Rodríguez Sánchez G (2007) Modeling epidemics using cellular automata. Applied Mathematics and Computation 186: 193-202.
45. Williams S, Oliker L, Vuduc R, Shalf J, Yelick K, Demmel J (2009) Optimization of sparse matrix-vector multiplication on emerging multicore platforms. Parallel Computing 35: 178-194.
46. Youssef M, Scoglio C (2011) An individual-based approach to SIR epidemics in contact networks. Journal of Theoretical Biology 283: 136-144.